FOSSIL IMPRINT • vol. 78 • 2022 • no. 1 • pp. 1–43

NATIONAL MUSEUM

ASSESSMENT OF PHYTOGEOGRAPHIC REFERENCE REGIONS FOR CENOZOIC VEGETATION: A CASE STUDY ON THE MIOCENE FLORA OF WIESA (GERMANY)

We dedicate this article to the memory of Professor Zlatko Kvaček (1937–2020), a world-leading and highly esteemed authority in Cenozoic palaeobotany.

LUTZ KUNZMANN[1,*], SHU-FENG LI[2], JIAN HUANG[2], TORSTEN UTESCHER[3,4], TAO SU[2], ZHE-KUN ZHOU[2,*]

[1] Senckenberg Natural History Collections Dresden, Königsbrücker Landstraße 159, 01109 Dresden, Germany; e-mail: Lutz.Kunzmann@senckenberg.de.
[2] Key Laboratory of Tropical Forest Ecology, Xishuangbanna Tropical Botanical Garden, Chinese Academy of Sciences, Menglun, Mengla, Yunnan, 666303, China; e-mail: zhouzk@xtbg.ac.cn.
[3] Senckenberg Research Institute and Natural History Museum, Senckenberganlage 25, 60325 Frankfurt/M, Germany.
[4] Institute for Geosciences, University of Bonn, Nussallee 8, 53115 Bonn, Germany.
*corresponding author

Kunzmann, L., Li, S.-F., Huang, J., Utescher, T., Su, T., Zhou, Z.-K. (2022): Assessment of Phytogeographic Reference Regions for Cenozoic vegetation: a case study on the Miocene flora of Wiesa (Germany). – Fossil Imprint, 78(1): 1–43, Praha. ISSN 2533-4050 (print), ISSN 2533-4069 (on-line).

Abstract: During the Miocene Climatic Optimum, a global long-term warm interval, European mid-latitude regions experienced a subtropical palaeoclimate. In particular, areas in eastern Germany were part of a vegetational zone with evergreen broadleaved forests, characterized by subtropical taxa. Regional palaeofloristic concepts denominated this palaeovegetation Younger Mastixioideae Flora sensu Mai (1964). Type assemblage is the late Early Miocene flora of Wiesa. Here, we reevaluate its floristic composition with respect to nearest living relatives of fossil-taxa, and introduce the new approach Phytogeographic Reference Region Assessment (PRRA) to ascertain the area of most similar extant vegetation for the Wiesa assemblage. The southern belt of SE Asian subtropical evergreen broadleaved forest and its transition to tropical mountain evergreen broadleaved forest in SW China represent the most similar extant vegetation. The Wiesa assemblage is compared to two diverse plant macro-assemblages from the late Oligocene and the Late Miocene, respectively, coming from the same region and palaeoenvironmental setting. It is demonstrated that diversity and abundances of subtropical taxa markedly increased towards the Early Miocene, and specific climate-sensitive taxa occurred. The regional palaeoclimate was subtropical-humid (Köppen-Trewartha type Cf), with a growing season eleven months long. The late Oligocene and Late Miocene climates were mainly distinct in nine-month growing season lengths and cooler winters (1–3 °C).

Key words: Phytogeographic Reference Region Assessment, Younger Mastixioideae Flora, Borna-Ost/Bockwitz, Wischgrund, Miocene Climatic Optimum

Received: June 8, 2021 | Accepted: November 30, 2021 | Issued: August 26, 2022

Introduction

Two phases of prominent subtropical palaeovegetation during the Cenozoic were recognized in central Europe, in particular from central Germany (e.g., Kirchheimer 1938, Mai 1964, 1995, Teodoridis and Kvaček 2015). These intervals coincide with long-term palaeoclimatic optima in the Paleogene and Neogene, respectively, that are called Early Eocene Climatic Optimum (EECO; e.g., Zachos et al. 2001, Inglis et al. 2020) and Miocene Climatic Optimum (MCO; e.g., Zachos et al. 2001, 2008, Steinthorsdottir et al. 2021). The latter was originally introduced as Mid-Miocene Climatic Optimum (e.g., Zachos et al. 2001, You et al. 2009) but modern age control places this warm interval between 16.9 Ma and 14.7 Ma (Holbourn et al. 2015), which is late Early to Middle Miocene (Early-Middle Miocene boundary: 15.97 Ma; Cohen et al. 2013). Westerhold et al. (2020) name the world's climate state during EECO "hothouse", the subsequent period until the Eocene-Oligocene Transition (EOT; Hutchinson et al. 2021) "warmhouse", and they characterize the Earth's climate state during the Oligocene and Miocene as "coolhouse". This classification means that the MCO is a less pronounced warm interval compared to the EECO. At about 13.9 Ma, the beginning of the Middle Miocene Climate Transition (mMCT; Flower and Kennett

DOI 10.37520/fi.2022.002

1994) marks the transition towards distinctly cooler phases (Westerhold et al. 2020).

EECO and MCO were defined in the marine realm, based on significant long-term (several million years) excursions of the oxygen isotope record, calibrated from deep-sea benthic foraminifera (Zachos et al. 2001, 2008, Westerhold et al. 2020). These changes in the isotopic composition primarily reflect changes in the average deep-ocean water temperatures, but are often used as global climate proxy. Although it is uncontroversial that ocean water temperatures and atmospheric state, and thus climate, are coupled, it became clear that regional climatic trends in the terrestrial realm could partly differ from the global oceanic history (e.g., Hutchinson et al. 2021). The EOT, for instance, is distinguished by a dramatic decrease in ocean water temperatures (Zachos et al. 2008). While in various studies, a strong coupling of marine and continental signals across EOT was reported (e.g., Mosbrugger et al. 2005, Donders et al. 2009, Ivanov et al. 2011), it is less pronounced or even undetectable in several regions on different continents observed from biotic proxies such as fossil plants (e.g., Pound and Salzmann 2017).

Miocene climate, atmospheric history and vegetational history have been focal research topics since the terminology of global palaeoclimatic intervals have been defined by the publications of Flower and Kennett (1994), and Zachos et al. (2001). Various papers on global- to continental-scale perspectives (e.g., Bruch et al. 2007, Bruch et al. 2011, Utescher et al. 2011, Pound et al. 2012, Teodoridis and Kvaček 2015, Li et al. 2018, Methner et al. 2020, Teodoridis et al. 2020) and regional-scale perspectives (e.g., Utescher et al. 1997, Kvaček et al. 2006, Erdei et al. 2012, Kovar-Eder and Teodoridis 2018, Bondarenko et al. 2019, Kovar-Eder et al. 2021) indicate that fossil plant assemblages are valuable proxies for terrestrial palaeoclimate reconstruction. Pound et al. (2012), for instance, used a 617-site palaeobotanical dataset, and stated that palaeoclimatic and palaeovegetational evolution was different between the hemispheres, probably based on the influence of the Antarctic icesheet on the Southern Hemisphere's climate. Furthermore, using the palaeobotanical record, it was found that throughout most of the Cenozoic, temperature gradients in the Northern Hemisphere were much shallower than today (e.g., Greenwood and Wing 1995, Fauquette et al. 2007, Utescher et al. 2011, 2017, Popova et al. 2017). It became also evident that, besides climate, atmospheric pCO_2 is a major force in vegetation changes during the Miocene (Kürschner et al. 2008, Steinthorsdottir et al. 2021).

In central Europe, several studies have been conducted to trace regional palaeoclimatic shifts during the MCO based on fossil plant assemblages (e.g., Mosbrugger et al. 2005, Teodoridis and Kvaček 2015, Doláková et al. 2021). Böhme et al. (2007) used fossil wood floras in southern Germany to detect two warmer phases in the middle Burdigalian and Langhian, and a marked cooling phase in the late Burdigalian, possibly caused by the second major Miocene built-up phase (Mi2) of the Antarctic icesheet.

Here, we use fossil diaspore and leaf assemblages from eastern Germany for a case study analysing the palaeophytogeographic and palaeoclimatic character of fossil assemblages in relation to the Miocene warm interval. For appropriate characterization of subtropical palaeovegetation in northern central Europe, the fossil flora of Wiesa in eastern Germany is of central importance. It has been called the "most subtropical" Miocene plant assemblage in central and eastern Germany (Mai 1995, 2000b, Kunzmann and Mai 2005). The Wiesa site near the town Kamenz in Saxony (Text-fig. 1) is a classical palaeobotanical locality, which became famous by its rich and diverse carpoflora (Kunzmann and Mai 2005). Based on his palaeofloristic considerations, Kirchheimer (1938) characterized the fossil assemblage as being derived from subtropical palaeovegetation, and named it Mastixioideae Flora, based on the abundance of prominent Mastixioideae (Nyssaceae) drops, a term that he extended to similar composed assemblages from other sites. The concept of Mastixioideae floras is a regional (German) perspective on the climate-driven evolution of regional vegetation in the Cenozoic that is, by content, partly similar to other floristic concepts such as the Palaeotropic Flora of Engler (1908, Mai 1995) for Europe, and the Poltava Flora of West Russia and Ukraine (Kryshtofovich 1929, Mai 1995). Based on an updated lithostratigraphic frame for the Paleogene and Neogene in central and eastern Germany, Mai (1964, 1967, 1995, 2000b) proposed a modified concept for Mastixioideae floras as follows, Early-Middle Miocene floras of the Wiesa type (including Wiesa) are Younger Mastixioideae floras, whereas similar floras from the Paleogene, mainly Eocene, could be called Older Mastixioideae floras (Mai 1995). Thus, Mastixioideae floras represent the typical mid-latitude palaeovegetation during the long-term palaeoclimatic optima in the Paleogene and Neogene (Mai 1995, Teodoridis and Kvaček 2015).

In the present paper, we reconsider and reevaluate the floristic composition of the Wiesa macrofossil plant assemblage being a proper proxy for mid-latitude palaeovegetation in northern central Europe during the MCO. Using the method Phytogeographic Reference Region Assessment (PRRA), which we introduce here as a new approach for quantitative determination of the most similar extant forest vegetation, we update the characterization of the local palaeovegetation. The results are compared to the outcome using another recently proposed similarity approach based on the Integrated Plant Record (IPR) Vegetation Analysis and Similarity Approach (Teodoridis et al. 2020, Kovar-Eder et al. 2021, Teodoridis et al. 2021). Furthermore, we use three different approaches to calculate palaeoclimate parameters under which the local palaeovegetation was growing. These approaches use nearest living relatives and/or ecological equivalents of fossil-taxa and their climatic preferences. In particular, we apply: (1) the Coexistence Approach (CA; Mosbrugger and Utescher 1997, Utescher et al. 2014); (2) the Bioclimatic Analysis (BA; Li et al. 2015); and (3) the Overlapping Distribution Analysis (ODA) approach (Yang et al. 2007) that has been earlier introduced as Isopore Approach (IA) by Mai (1995).

To demonstrate distinctiveness of the palaeovegetation and to estimate the palaeoclimatic characteristics during the late Early Miocene in a regional context, the Wiesa assemblage is compared to the older, i.e., late Oligocene, Borna-Ost/Bockwitz TC flora and the younger, i.e., Late Miocene, Wischgrund flora, based on new and recently published data (Kvaček and Walther 2001, Striegler 2017,

Moraweck et al. 2019). Both diverse macrofloras represent palaeovegetation and palaeoclimatic conditions before and after the MCO, respectively (Mai 1995), which is inferred from their lithostratigraphic positions (Standke et al. 2010, Escher et al. 2020). Both assemblages come from depositional palaeoenvironments, i.e., fluvio-alluvial siliciclastic units deposited in costal lowlands (Standke et al. 2010, Escher et al. 2020), similar to the setting of the assemblage of Wiesa (Escher et al. 2020).

The Wiesa fossil site

Geological and stratigraphical background

The plant fossils of Wiesa were recovered from fluvio-alluvial deposits in the vicinity of the city of Kamenz (Sachsen, eastern Germany; Text-fig. 1). These deposits are part of the Neogene coastal plain sedimentary sequences of the NW-German-Polish Basin (Escher et al. 2020), but they are actually an isolated erosional remnant of a formerly closed sediment cover. According to palaeogeographical reconstructions by Standke (2008) and Escher et al. (2020), the site was approximately 10–15 km inland from the coastline of the Palaeo-North Sea. The present-day Earth's surface outline of the deposits, which are about 4 km long and 1.5–2 km wide, clearly refers to accumulations of a river in a S to N oriented alluvial plain. Isolation of these local deposits from the Neogene sediment series to the North, as well as heterogeneity and low lateral expansion of individual sediment beds in fluvial siliciclastic sequences still raise questions about the lithostratigraphic correlation of the Wiesa section with the regional standard section. The upper part of the Wiesa section, as exposed in the kaolin quarry of Wiesa (Text-fig. 2), shows deformed, slightly folded sediments that are indicative of movement of Pleistocene glaciers.

The general lithological section exposed in the Wiesa kaolin quarry starts with kaolinized Proterozoic granodiorite in autochthonous stratification (Escher et al. 2020). This part of the kaolin lagerstätte is overlain by allochthonous kaolin strata that were transported by rivers for a certain distance. Both horizons are free of fossils. Above the kaolin lagerstätte, a fluvio-alluvial siliciclastic complex, including one or two thin lignite seams, terminates the Miocene sedimentary sequence. Historical reports always point to a single thin lignite seam. However, what is currently exposed at the southern highwall of the quarry is a multilayered complex subdivided into two lignite seams and a thin siliciclastic interburden. The lithostratigraphic position of the thin lignite seams is commonly assumed to be equivalents of the 2nd Miocene Lignite Seam Complex, which is lower Langhian (Middle Miocene) in age (Escher et al. 2020). However, due to the marginal position of the Wiesa lignite within the coastal swamps, an exact correlation with the standard section of the seam complex is currently not possible (pers. comm. Dr. Jochen Rascher, GEOMONTAN GmbH company, Freiberg/Sa., Germany). Fossil plant remains have been washed out over decades from a tens-of-meters wide but a few meters thick lens-like depositional structure beneath the lignite seams. However, this structure is currently not exposed, or it has already been completely removed by the excavation process. Neither do exact descriptions of the sediments exist, nor any proper sediment sample for a sedimentological analysis. These facts complicate a precise denomination of the architectural facies type of the fossil-bearing horizon. According to Walther (1984), only a single channel deposit was the subject of sampling of fossil material within a timespan of 4–5 decades. Likely, the Wiesa flora is an assembled taphocoenosis, but palaeocarpological investigation revealed no hint that it encompasses fossils from different palaeofloristic phases (Mai 2000b). Lithostratigraphically, the complete Neogene Wiesa section covers presumably parts of the Lübbenau Member of the Spremberg Formation (lower Burdigalian; Escher et al. 2020) and parts of the Brieske Formation (Text-fig. 3; Escher et al. 2020). Thus, a maximum age range for the complete section is appr. 20 to 14 Ma (complete Burdigalian and lowermost Langhian; Escher et al. 2020). Most likely, the fossil-bearing bed(s) beneath the lignite seam belong to the Drebkau Member of the Brieske Formation, which is middle Burdigalian in age (18–16.5 Ma; Escher et al. 2020), which is in agreement with the former assumption of Mai (2000b). According to the palynological zonation of central and eastern Germany, Wiesa was dated to the Spore-Pollen-Neogene (SPN) zones VI A to C, and likely VII, which also corresponds to a middle to late Burdigalian age (Krutzsch 2000). However, the biostratigraphic position is not proven by any non-pollen palaeontological data (pers. comm. late W. Schneider, Hoyerswerda, Germany). Thus, the assumed age range of the Wiesa plant assemblage does not completely fit into the MCO range, which is 16.9 Ma to 14.7 Ma (e.g., Steinthorsdottir et al. 2021), but merely corresponds to its beginning.

Floristic composition, palaeoenvironment and palaeoclimate

The Wiesa assemblage contains 120 taxa of fossil plants whereof 16 taxa are gymnosperms, 2 taxa are pteridophytes and all others are angiosperms (Apps I, II). Most of the taxa are elements of the zonal vegetation, and intrazonal (azonale) elements are minor components (Mai 2000b). The floristic analysis refers to an ecotone between diverse mixed mesophytic forest (MMF) and evergreen broadleaved forest (EBF), with a clear relationship to extant East Asian EBF (Mai 2000b). By contrast, Teodoridis and Kvaček (2015) conducted an Integrated Plant Record analysis (IPR; Kovar-Eder and Kvaček 2007, Kovar-Eder et al. 2008, Teodoridis et al. 2011) based on Mai's (2000b) taxon list, which is given in revised form herein (Apps I, II), and assign the Wiesa assemblage to an evergreen broadleaved forest (EBF). Several other Early Miocene and Early Middle Miocene floras of eastern Germany and the northern regions of the Czech Republic are characterized as EBF as well (Teodoridis and Kvaček 2015).

Specifically, Mai (2000b) pointed out the predominance of subtropical taxa of the (sub-)families Mastixioideae, Symplocaceae, Lauraceae, Theaceae, Sabiaceae, Rutaceae, Euphorbiaceae and others. This type of a diverse Younger Mastixioideae Flora typically contains fossil-species of *Eomastixia*, *Mastixicarpum* (*Diplopanax*), *Retinomastixia*,

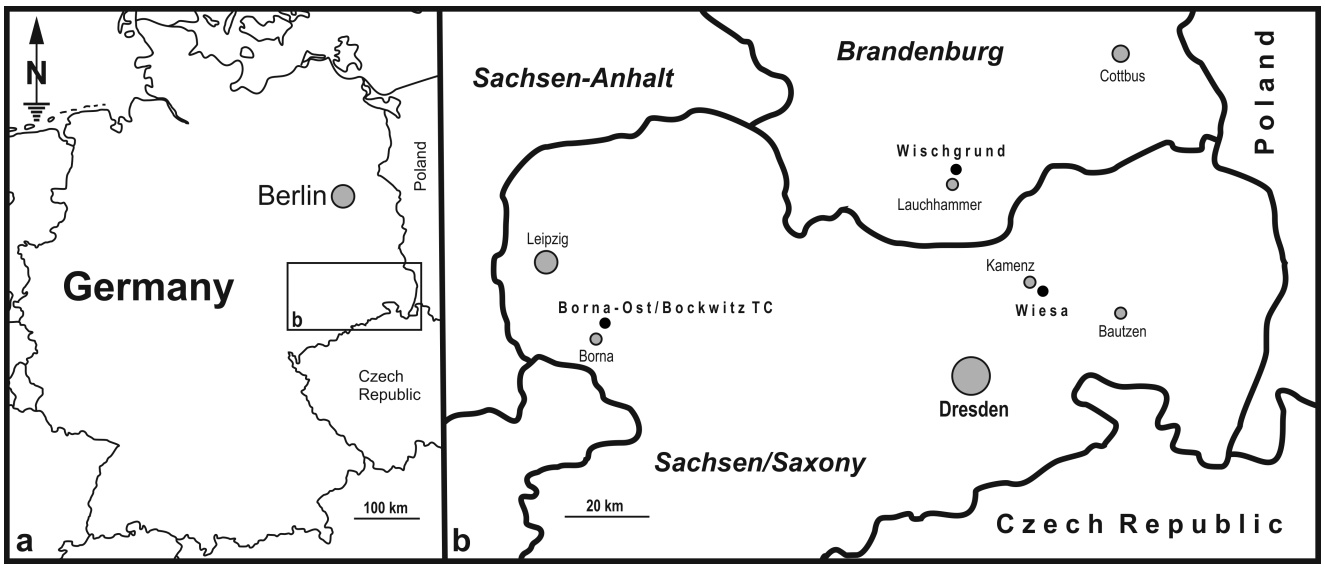

Text-fig. 1. Location of Wiesa fossil site in eastern Germany and other fossil sites for comparison. Explanation for map b: all fossil sites – black circles; grey circles – cities; topographic names in italics – German states (Länder). For bio- and lithostratigraphic data of fossil sites, see chapter Methodologies and material and Text-fig. 3.

and *Tectocarya*, making it distinctive from other floras of this region (Mai 2000b).

A preliminary palynological analysis was conducted by Vomela (2016), using a sample from uncontrolled und undated sampling. Investigations confirmed the general palaeoecological and palaeophytosociological interpretations of the Wiesa flora based on the macrofossil record (Mai 2000b). Important presence/absence data of palynomorphs as recorded by Vomela (2016) will be discussed below.

Based on his floristic analysis, Mai (2000b) assumed the following palaeoclimate parameters by using average climate data from central and southern P. R. China where EBF is growing: climate type Cfa after the Köppen-Geiger classification (Köppen 1936); warm-temperate and humid climate with hot but not dry summers, rare frosts; mean annual temperature (MAT): 18–21 °C; mean temperature of the coldest month (CMMT): 4–10 °C; mean temperature of the warmest month (WMMT): 25–28 °C; mean annual precipitation (MAP): 800–2,000 mm. Mai (2000b) also concluded that the climate reconstructed for Wiesa obviously indicates the beginning of the global Miocene Climatic Optimum. Teodoridis and Kvaček (2015) confirmed Mai's (2000b) palaeoclimatic interpretation by using the Coexistence Approach (for methodology see below).

A single fossil-species of the Wiesa assemblage, *Laurophyllum pseudoprinceps* (Lauraceae), was used by Grein et al. (2013) for calculation of the palaeoatmospheric pCO_2 values, applying mechanistic gas-exchange modelling (Konrad et al. 2008). The result, 399–780 ppm pCO_2, is in accordance with other proxy data for the onset of the MCO (Grein et al. 2013).

Text-fig. 2. Kaolin clay pit at hill Hasenberg in Wiesa, Saxony, Germany; view of southern high wall, showing deeply weathered late Early Miocene lignite seam by dark brown color in center (photographed 2015). Fossil-bearing strata were reported (e.g., Mai 1964) as below lignite seam, but this horizon does actually not crop out (also evidenced by new drillings, communicated by Dr. Jochen Rascher, GEOMONTAN GmbH company, Freiberg/Sa., Germany).

Methodologies and material

Phytogeographic Reference Region Assessment (PRRA)

The method that we introduce here basically takes up palaeobiogeographic considerations by Mai (1995) for palaeoclimate reconstructions denominated Isopore Approach (IA). In this graphical approach, the distribution areas of nearest living relatives (NLR; e.g., Uhl et al. 2003) of fossil-taxa are drawn in maps to construct an area in which most of the NLRs co-occur (Mai 1995). Margins of these intersection or overlap areas are called isopores, a term introduced by Rothmaler (1938). By definition, an isopore borders areas of equal number of taxa co-occurring in that area (Mai 1995). Consequently, applied to a fossil flora, one should receive several overlap areas likely in different parts of the world. Furthermore, Mai (1995) states that climate in an overlap area in which most of the NLRs

co-occur could serve as proxy for the palaeoclimate at the fossil site. Values of climate parameters have to be obtained from climate diagrams from meteorological stations within or in proximity to the selected cut set area. Applied to fossil floras, IA will provide in many cases more than one cut set area and thus more than one set of climate proxy data (Mai 1995). Therefore, Mai (1995) recommended to combine IA with a vegetational analysis, which should gather climate data from an extant vegetation that is most similar to the fossil assemblage in terms of floristic composition. Thus, Mai's (1995) approach is a deductive method and requires profound floristic knowledge. The same method has been re-introduced by Yang et al. (2007) as Overlapping Distribution Analysis (ODA).

Another, slightly different approach was proposed by Andreánszky (1959). He suggested reconstructing an extant "ecological area", in which most of the modern relatives of a fossil flora could co-exist. The selection of modern relatives therein is based on ecological demands and not primarily on taxonomic relationships. Kunzmann et al. (2016) and others call this extant taxon "ecological equivalent", which could be distinct from the NLR. Ecological equivalents (EE) could replace NLRs in cases when the fossil-species belongs to extinct genera and families, which makes selections of reliable NLRs almost impossible. In short, all the above-mentioned methods are based on the derivation of an extant area in which NLRs or EE can coexist, and prevailing climate conditions in that area serve as proxy for palaeoclimate reconstructions. None of the authors of these approaches proposed to utilize the methodologies of overlapping areas for searching for the most similar extant vegetation of a fossil assemblage, which we do here.

To semi-quantitatively compare a fossil flora with extant vegetation types and to conclude on reference regions with most similar extant vegetation, we propose a new graphical approach that also utilizes NLRs and EEs and their distribution data. We name this approach Phytogeographic Reference Region Assessment (PRRA), and it is based on calculating the number of identical genera that are found both in a fossil flora and in modern vegetation data, plotted in a latitude/longitude grid. Distribution data of modern taxa are utilized from the open access Global Biodiversity Information Facility database (GBIF, www.gbif.org). The new approach can be conducted when using a script written with R® software package (App. III). General working steps, here applied to the flora of Wiesa, are as follows:

1. Identification of NLRs or EEs of the taxa in a fossil flora.
2. NLRs and/or EEs are selected and grouped into a coarse regional system indicating the modern distribution, such as E and SE Asia, N America, Europe, cosmopolitan; SE Asia + N America etc. (for Wiesa see App. II).
3. The region where most of the NLRs/EEs occur is selected; here it is E/SE Asia. Further analysis is conducted with the selected part of NLRs/EEs.
4. Occurrence data of the NLRs/EEs taxa are downloaded from GBIF. Subsequently, data is cleaned following the method described by Palazzesi et al. (2014).
5. Using the R® script, distribution data are illustrated in grid boxes. Here, we run the analysis with 1°, 1.5°, 2° and 3° latitude/longitude resolution.
6. The grid box(es) with highest occurrences of NLRs/EEs are denominated as reference grid box(es).
7. If available, climate-sensitive fossil-taxa and their NLRs are additionally used for qualitative determination of a reference region encompassing the grid box(es).
8. The extant reference vegetation unit is ascertained from modern vegetation maps.

Integrated Plant Record (IPR) Vegetation Analysis and Similarity Approach

For comparison with our results from the PRRA approach, we conducted an IPR Vegetation Analysis (Kovar-Eder and Kvaček 2007, Kovar-Eder et al. 2008, Teodoridis et al. 2011). IPR is a semi-quantitative tool for reconstructing major zonal vegetation units from fossil assemblages, based on the classification of the fossil-taxa into 13 taxonomic-physiognomic components (Teodoridis et al. 2011). Recently, two new tools, Drudge 1 and 2 have been introduced to determine modern vegetation proxies for fossil assemblages, called Similarity Approach (Teodoridis el al. 2020, 2021). Another tool, denominated Taxonomic Similarity, estimates which extant vegetation units are taxonomically most similar to the fossil flora. The tools utilize similarities in the proportions of zonal key elements and taxonomic similarity between fossil assemblages and a calibration dataset of (currently 505) modern vegetation units from Europe and Asia (the Caucasus region, Mongolia, China, Japan) (Teodoridis el al. 2020). IPR Vegetation Analysis and Similarity Approach can be conducted online using a freely accessible database: http://www.iprdatabase.eu (Teodoridis et al. 2011–2021), which was recently expanded to include the Drudge 1 and 2 tools (Teodoridis et al. 2020–2021). The online database provides a score sheet template that can be used for scoring the fossil-taxa of an assemblage regarding its taxonomic-physiognomic classification. When uploading the completed score sheet, one will receive the detailed results of the IPR Vegetation Analysis, including results for the Similarity Analysis Drudges 1 and 2, for Taxonomic Similarity and for Result-Mixes Drudges 1 and 2. We have submitted our score sheet for the flora of Wiesa to the website administrator for inclusion in the online database. It is accessible when exploring the database and can be used for running an IPR Vegetation Analysis and Similarity Approach.

Climate classification systems

Vegetation zones on Earth correspond to climate zones and vice versa. Each climate zone can be characterized by a specific climate type that is the aggregated set of climatic parameters, such as temperature, precipitation, and seasonal shifts of both. When characterizing the palaeovegetation of Wiesa based on the most similar vegetation types, it is accepted that similar vegetation also indicates a similar climate type. Two climate classification systems are commonly used, i.e., Köppen-Geiger (Köppen 1900, 1936, Geiger 1954) and Köppen-Trewartha (Belda et al. 2014).

The Köppen-Geiger classification system (Köppen 1936, Geiger 1954) distinguishes five main climate types on Earth: tropical (A), dry (B), temperate (C), continental (D), and polar (E). The main types are further subdivided

into precipitation types, indicated by the second letter, and temperature levels of two 6-months periods during the year (summer and winter), indicated by the third letter.

The Köppen-Trewartha classification system (Trewartha 1968, Trewartha and Horn 1980) is based on the classical classification, but gives more attention to distinguishing wet and dry climates, which makes this system correspond better to natural landscape boundaries (Belda et al. 2014). In our opinion, the Köppen-Trewartha classification system could be a better tool for characterization of Paleogene and Neogene climate types, as it distinguishes tropical (A), subtropical (C) and temperate (D) climate types, based on mean monthly temperatures (MMT) and the number of months per year with MMT values above or below certain limits (Belda et al. 2014). Besides, the system also specifies boreal (E), polar (F) and dry climate type (B) groups. The second letter in the Köppen-Trewartha classification system refers to specific temperature values, or in case of group B, to precipitation patterns. This classification system is particularly useful for characterization of Miocene climate types in central Europe, i.e., whether they were true subtropical or (warm-)temperate. The Köppen-Trewartha classification system separates subtropical from temperate climate by the number of months with MMT > 10 °C, which is the crucial limit for plant growth, meaning that the number of months correspond to the length of the growing season (Belda et al. 2014). Grein et al. (2013) proposed a simple equation to calculate MMT from Coexistence Approach (see below) data and use these MMT values for reconstruction of the growing season length. MMT for each month is calculated as follows:

$$T = A \sin\{(M+8)\pi/6\} + MAT$$

with MAT – mean annual temperature, M – number of months, A – half distance between WMMT and CMMT.

Approaches for palaeoclimate reconstructions

Initially, it needs to be stated that geological sections of unconsolidated siliciclastic sediments that include lignite frequently are de facto without any animal fossil, because all hard parts of invertebrates and vertebrates are usually dissolved by migrating humic acids (e.g., Kunzmann et al. 2017). That is why other biota-based palaeoclimate reconstruction techniques are not applicable. Currently, this is also the case for the Wiesa site, for which only plant fossils can be utilized for quantitative palaeoclimatic reconstructions.

Coexistence Approach (CA)

The meaningfulness of this method has been the subject of controversy recently, because of methodological limits and uncertainties (e.g., Grimm and Denk 2012, Utescher et al. 2014). Nonetheless, for assemblages such as Wiesa, which mainly consist of non-leaf fossil remains, there is no real alternative to CA, since leaf physiognomic approaches such as Leaf Margin Analysis (Wolfe 1979, Su et al. 2010) and Climate Leaf Analysis Multivariate Program (CLAMP; Wolfe 1993, Spicer et al. 2009, Yang et al. 2011) only provide reliable results if sufficient numbers of taxa and/or morphological leaf types are available. From Wiesa, only 8 angiosperm taxa have been determined from the leaf component (unpublished results of LK). The theoretical background of CA (Mosbrugger and Utescher 1997, Utescher et al. 2014) is related to the concept of the NLRs and the actualistic assumption that climatic requirements of extant plants could directly serve as a proxy for climatic requirements of fossil-taxa (Wing and Greenwood 1993, Mosbrugger 1999, Uhl et al. 2003). In most cases, the most similar (morphology and anatomy) extant taxon (genus or even species) is selected because a direct phylogenetic relationship between extant and fossil-taxa cannot easily be proven. The advantages of CA are that not only leaves but also taxa based on wood, diaspores and pollen can be incorporated in the analysis (Utescher et al. 2014), and the method is supposed to be therefore more independent from taphonomic biases (Uhl 2006) than leaf physiognomic approaches. In short, CA determines an interval of coexistence of climate requirements of all NLRs or most similar extant taxa that are known for a fossil flora. CA gives values for several climatic parameters such as MAT, warmest month mean temperature (WMMT), coldest month mean temperature (CMMT), mean annual precipitation (MAP), mean precipitation of the driest month (MPdry), mean precipitation of the wettest month (MPwet) and others. The climatic parameters of the NLRs were taken from the PALAEOFLORA database (Mosbrugger and Utescher 1997, PALAEOFLORA 2018). Fossil taxa and their assumed NLRs for the flora of Wiesa are provided in Appendix 2.

Bioclimatic Analysis (BA)

The Bioclimatic Analysis (BA; Kershaw 1997, Eldrett et al. 2009, Reichgelt et al. 2013, Li et al. 2015) is additionally applied to calculate palaeoclimatic variables. BA is modified from CA, and has recently been successfully applied by a number of researchers in palaeoclimate reconstruction (Palazzesi et al. 2014, Li et al. 2015, Prebble et al. 2017). Both BA and CA use the climatic envelopes of the NLRs of fossil taxa to derive the values of palaeoclimate parameters, but the difference between these approaches is how they define the climatic ranges: CA uses the minimum to maximum values of parameters of modern climate data derived from the distribution area of each taxon, while BA uses the 10^{th} to 90^{th} percentiles of the climate data to determine the climatic envelope (Thompson et al. 2012). BA thus removes statistical outliers and so increases the precision of the estimated palaeoclimate data (Li et al. 2015).

Isopore Approach (IA) and Overlapping Distribution Analysis (ODA)

Both IA (Mai 1995) and ODA (Yang et al. 2007) are based on utilization of distribution data of NLRs of fossil-taxa, resulting in an area where most of the distribution areas of NLRs overlap ("maximum overlap" in Yang et al. 2007). Climate proxy data come from a meteorological station associated with the overlap area (Mai 1995, Yang et al. 2007). Herein, climate data for the reference grid box revealed from PRRA are collected from the online resource CLIMATE-DATA.org. Climate data are model data

based on data of the European Centre for Medium-Range Weather Forecasts (ECMRWF; operating EU's Copernicus Atmosphere Monitoring Service and the Copernicus Climate Change Service).

Short characteristics of compared sites and assemblages

To evaluate how distinct palaeovegetation and palaeoclimate of the Wiesa site from older and younger assemblages is, i.e., assemblages that clearly represent pre-MCO and post-MCO vegetation, two rich and diverse macro-fossil assemblages from eastern Germany were chosen for floristic comparison. Our selection was based on the following preconditions: (1) palaeogeographic position in the coastal lowlands to have an equal climatic signal (e.g., the influence of oceanity), (2) similar fluvio-alluvial habitat deduced from the depositional facies type and regional geological data, (3) diverse assemblages containing both carpological and leaf remains, (4) distinct stratigraphic ages in relation to the MCO time interval based on settled lithostratigraphic and phytostratigraphic positions. Following these preconditions and based on published datasets we have chosen the following sites.

Borna-Ost/Bockwitz TC represents a flora of the early late Oligocene "deterioration" phase (Kvaček and Walther 2001, Teodoridis and Kvaček 2015), distinctly before the beginning of MCO, and the Late Miocene Wischgrund flora displays the global cooling phase in the Late Miocene (after the beginning of mMCT; Mai 1995).

The plant assemblage of **Borna-Ost/Bockwitz TC** (NW Sachsen, Germany; Text-fig. 1) combines several taphocoenoses from the basal part of the fluvial Thierbach Clay Complex, Thierbach Member, Cottbus Formation in the central German Leipzig Embayment (Text-fig. 3; Mai and Walther 1991, Standke et al. 2010). Individual sampling sites were chosen in the abandoned lignite opencast mines Borna-Ost and Bockwitz, collected between 1973 and 1996 (Mai and Walther 1991; own field work). Krutzsch (2011) correlated the fossiliferous horizon with the regional Spore-Pollen-Paleogene zone 20I, corresponding to a lower Neochattian (upper Oligocene) age, approximately 25.5–24.5 Ma. Fossil taphocoenoses, classified as being mainly parautochthonous by origin, come from several abandoned channel fills (Gastaldo et al. 1996). Palaeoclimate estimation calculated warm-temperate and humid conditions; in particular CA provides MAT 15.7–16.1 °C, WMMT 25.4–25.6 °C, CMMT 5.0–6.2 °C, MAP 1,231–1,355 mm, whereas CLAMP values indicate distinctly cooler climate MAT 10.1 °C (± 1.3), WMMT 22.6 °C (± 1.7), CMMT –1.8 (± 2.6), growing season precipitation (GSP) 878.4 mm (± 497), precipitation of the three wettest months (3_wet) 591.8 mm (± 239), precipitation of the three driest months (3_dry) 134.7 (± 104) (Moraweck et al. 2019). These estimates are accepted herein; we refrain from another calculation. The IPR vegetation analysis, conducted by Teodoridis and Kvaček (2015), revealed mixed mesophytic forest (MMF), or an ecotone between MMF and EBF. The revised taxon list used herein was published by Moraweck et al. (2019), and is based on Mai and Walther (1991) and unpublished data by Walther and Kunzmann.

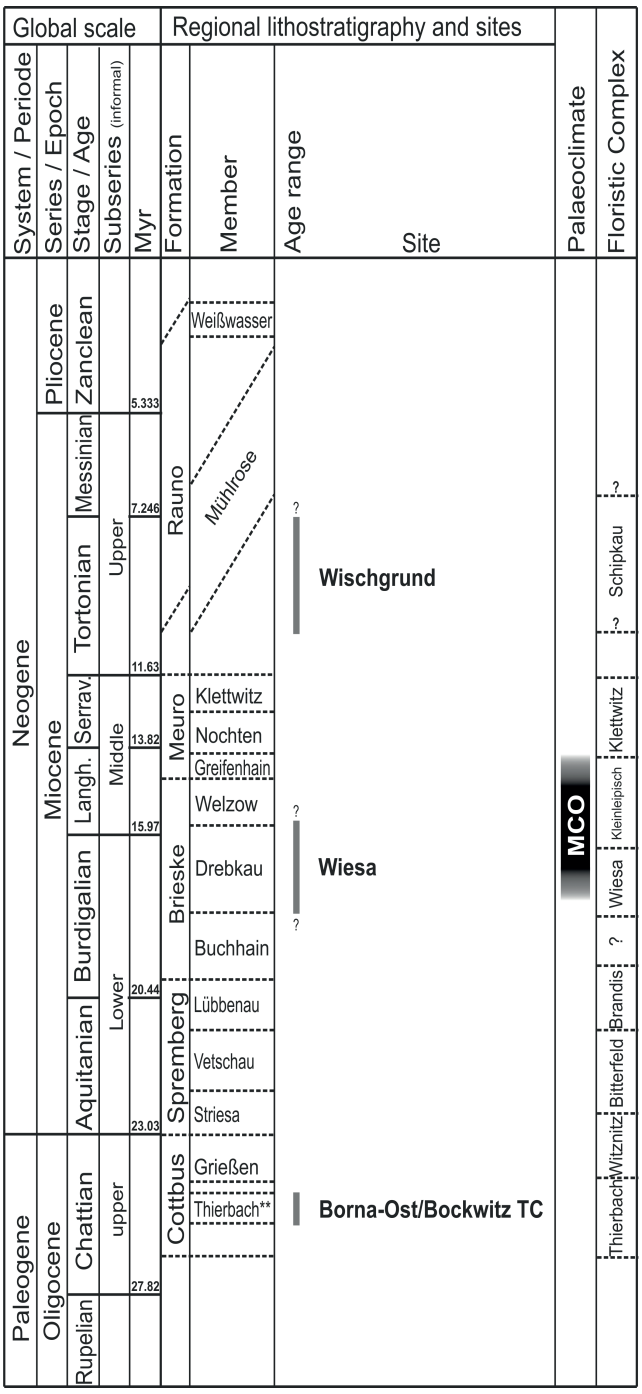

Text-fig. 3. Litho- and biostratigraphic position of fossil floras treated herein, based on lithostratigraphic standard section of upper Oligocene and Miocene in central and eastern Germany (Standke et al. 2010, Escher et al. 2020); only exception from standard section: ** – Thierbach Member restricted to central Germany, replaces Branitz Member in eastern Germany; correlated to global scale of International Chronostratigraphic Chart 2022/02 (Cohen et al. 2013); maximum age ranges of sites/floras indicated by black bars; floristic complexes according to definitions by Mai and Walther 1991 for upper Oligocene, Mai 2000b, 2001b for Miocene; age range of MCO from Steinthorsdottir et al. 2021.

The **Wischgrund** flora was collected from a site in SE Brandenburg, Germany (Text-fig. 1). Lithostratigraphically, the fossil site belongs to the Mühlrose Member of the Rauno Formation (Text-fig. 3). Regional lithostratigraphic

concepts, macrofloristic evaluation with respect to regional floristic complexes (Mai 2001b) and palynological datasets (regional Spore-Pollen-Neogene zone XXVI; Krutzsch 2000) place the Wischgrund layer into the middle Tortonian to Messinian (appr. 10–5 Ma). Escher et al. (2020) consider a middle to upper Tortonian age. The macro- and microflora was recently revised and analysed by Striegler (2017), using the IPR vegetation analysis tool. The Wischgrund flora represents a MMF with a high abundance of temperate deciduous elements, whereas evergreen taxa are comparatively rare (leaf taxa 14 %, carpological taxa 22 %, palynomorph taxa 11 %; Striegler 2017). Mai (2001b) included the Wischgrund flora into his Late Miocene floristic complex Schipkau, and gives the following palaeoclimatic estimations: MAT 13–15 °C, WMMT 24.5 °C, CMMT –2.7 °C (regular frosts and absolute minimum –15.5 °C), MAP 1,300 mm. By contrast, Teodoridis and Kvaček (2015) selected a coeval flora of the Schipkau floristic complex, the Klettwitz-12 assemblage of Mai (2001b) for calculating palaeoclimatic parameters as follows: MAT 15.7–16.3 °C, WMMT 25.7 °C, CMMT 4.7–6.2 °C, MAP 979–1,355 mm. Their IPR vegetation analysis for Klettwitz-12 revealed a deciduous broadleaved forest (DBF).

Material

For our analyses, we have used most recent publications of the fossil floras and their interpretations, namely (1) for the site Wiesa: Mai (1999a, b, 2000a, b), Kunzmann and Mai (2005); (2) for the site Borna-Ost/Bockwitz-TC: Mai and Walther (1991) and an unpublished revision by Walther and Kunzmann; and (3) for the site Wischgrund: Striegler (2017). All published lists of the fossil floras were revisited and if necessary, revised, based on updated knowledge of the taxa (Apps I, II). The same was conducted for the NLRs as well as the most similar extant species in cases of extinct genera.

List of abbreviations

BA	Bioclimatic Analysis
BLD	broadleaved deciduous component
BLE	broadleaved evergreen component
CA	Coexistence Approach
CLAMP	Climate Leaf Analysis Multivariate Program
CMMT	coldest month mean temperature
DBF	deciduous broadleaved forest
EBF	evergreen broadleaved forest
EE	ecological equivalent
EECO	Early Eocene Climatic Optimum
EOT	Eocene-Oligocene Transition
GSP	growing season precipitation
IA	Isopore Approach
IPR	Integrated Plant Record analysis
LEG	legume-like component
MAP	mean annual precipitation
MAT	mean annual temperature
MCO	Miocene Climatic Optimum
mMCT	middle Miocene Climate Transition
MMF	mixed mesophytic forest
MPdry	mean precipitation of the driest month
MPwet	mean precipitation of the wettest month
NLR	nearest living relatives

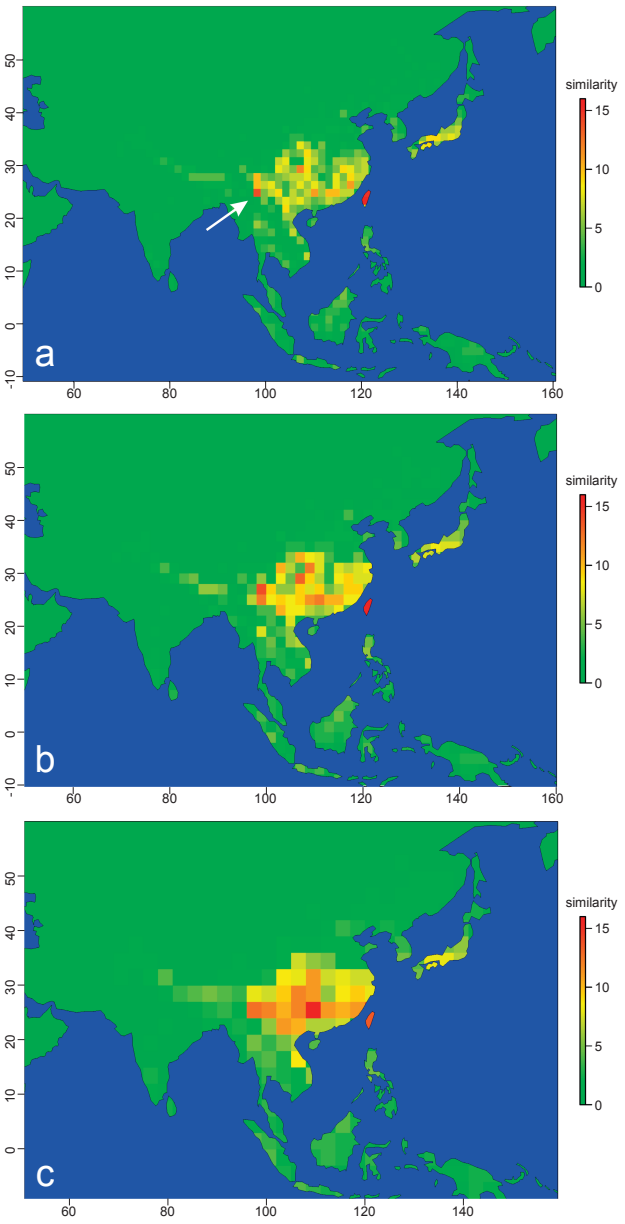

Text-fig. 4. Graphical visualization of Phytogeographic Reference Regions Assessment (PRRA) of nearest living relative genera of fossil-taxa from late Early Miocene Wiesa assemblage in eastern Germany. Analysis yields only NLRs which have modern distribution area (partly) in E and SE Asia. For relationships of fossil-taxa to nearest living relatives or ecological equivalents, see Tab. 6; taxa used for analysis marked with asterisks. Three geographic resolutions conducted: a – grid with 1.5° latitude/longitude resolution, b – grid with 2°, c – grid with 3°; similarity column indicates co-occurrences of genera of nearest living relatives in single grid box. Maximum value in our analysis: grid box marked with arrow in map a, located in western Yunnan Province, P. R. China and southern Kachin Province, NE Myanmar (east of Myitkyina city), area with 97.371 7–98.874 2° longitude and 24.586 7–25.837 5° latitude, yields 23 co-occurring species of 13 genera (Tab. 7).

ODA	Overlapping Distribution Analysis
PRRA	Phytogeographic Reference Region Assessment
SCL	sclerophyllous component
WMMT	warmest month mean temperature

Results

Phytogeographic Reference Region Assessment (PRRA) for Wiesa flora

Revisiting and compiling the assumed NLRs/EEs of the fossil-taxa in Wiesa revealed that almost half of the taxa (55) have clear relationships to genera and species in E and SE Asia (Tabs 1, 2). Only 13 taxa show a similarly clear relationship to North American species. Three fossil-taxa show relationships at the generic level to genera with a disjunct North American and E/SE Asian distribution, but more detailed comparisons on the species level to ascertain whether the fossil-species is more closely related to North American or E/SE Asian species are impossible at the moment. Five fossil-species are closely related to relics in the Mediterranean and Macaronesian floras, respectively. The remaining fossil-taxa show an unspecific relationship to extant taxa (Tab. 1). It must be mentioned that one-fifth (24) of the fossil-taxa cannot be related to any extant genus or group, either because they are extinct (e.g., *Sphenotheca*), or because the fossil taxonomic units are artificial groups of morphotypes such as *Daphnogene* (Lauraceae). Following the guidelines, the PRRA is conducted by using E and SE Asian taxa of the NLRs/EEs only. Taxa for which GBIF data are utilized are marked in Tab. 2. These taxa are 34 species of 32 genera and 5 taxa on a generic level. For the remaining taxa, GBIF data could not be utilized in proper quality.

The graphic results (Text-fig. 4) show that most of the grid boxes with high co-occurrence values are in South China, Taiwan Island, and in the northernmost parts of Vietnam and Myanmar. Grid boxes with highest values (colored red in Text-fig. 4) are in southwest China and Taiwan Island. Different grid resolutions reveal different quality of data. The 3° grid resolution analysis provides a rather wide area of similar vegetation encompassing most of the southern subtropical EBF zone from the coast to western Yunnan, and the southern part of the middle subtropical EBF zone (Text-fig. 4c). The highest values per grid box range between 15 and 20 taxa. By contrast, when applying the 2° grid resolution, this area falls to several subareas with high values (up to 16 taxa per grid box; Text-fig. 4b) interrupted by subareas with values <11 taxa. These high-co-occurrence grid boxes are situated in western Yunnan, Hubei, Hunan, Guangxi and Guangdong provinces. The 1.5° grid resolution reveals, besides Taiwan Island, 4 distinct areas with co-occurrence values >10 taxa, i.e., western Yunnan, eastern Guangxi, Fujian and northernmost Guizhou (Text-fig. 4a), with the western Yunnan area as highest similarity region. The grid box with highest co-occurrence of NLRs is situated in the westernmost part of Yunnan Province, north of Dehong city, west of Baoshan city, south of Nujiang city, and partly in the southern part of Kachin Province, NE Myanmar (east of Myitkyina city), an area with 97.371 7–98.874 2° longitude and 24.586 7–25.837 5° latitude (Text-fig. 4a: arrow). This reference grid box yields 23 species of 13 genera (Tab. 7), but the number of co-occurring taxa must be reduced to 16, because some NLRs are only defined on the generic level (*Calamus*, *Polyspora*, *Symplocos*; Tab. 2). Finally, a 1° grid resolution provides only grid boxes with co-occurrence values up to 8 taxa per box, and so is not considered here to be a useful result of the analysis.

Based on this analysis, the reference region for the fossil assemblage of Wiesa is concluded to be in southern to southwestern P. R. China, and to minor extent in northwestern Myanmar and northern Vietnam. According to the vegetation map of the P. R. China (Editorial Committee of Vegetation Map of China, The Chinese Academy of Sciences 2007), the reference region is mainly part of the subtropical evergreen broadleaved forest zone in southern P. R. China, but extends also into the northern tropical forest zone. The EBF biome in E Asia can be subdivided into four subzones or belts (Text-fig. 5) that are indicative areas for climate-sensitive species. Table 7 gives the list of climate-sensitive fossil-species from Wiesa, their assumed NLRs, and the subzone(s) in which the NLR is most abundant. Therefore, the extant reference vegetation unit is determined as the middle and southern belts of EBF, including a minor overlap with the tropical forest zone (Text-fig. 5). Based on the validity of climate-sensitive species, the high-co-occurrence-value grid boxes in the center of the middle subtropical EBF zone (Text-fig. 4a) are considered outliers from this assumed reference region and vegetation unit.

IPR Vegetation Analysis and Similarity Approach for Wiesa flora

The proportions of zonal taxa in the fossil flora of Wiesa are as follows: 82 of 120 taxa are zonal taxa, of which 62 taxa are woody angiosperms. Thereof, 45.16 % belong to BLD, 45.97 % to BLE, and 8.87 % to SCL+LEG (for acronyms see list of abbreviations in chapter Methodologies and material). Besides, zonal herbs constitute 4.85 % of zonal taxa. According to the scheme of Teodoridis et al. (2011), EBF is considered the major zonal vegetation type.

The Similarity Drudge 1 tool estimates “Broad-leaved Evergreen Sclerophyllous Forest (Guizhou)” as most similar extant vegetation unit, with a mathematical difference of 6.74 %; other vegetation units showing lower similarities occur in the Caucasus region and in Japan. The Similarity Drudge 2 tool delivers three most similar extant vegetation units in SE Asia: “Montane Coniferous Forest – Taiwan”, “Broad-leaved Evergreen Sclerophyllous Forest – Pine Forest (Yunnan)”, and “Broad-leaved Evergreen Sclerophyllous Forest (Guizhou)”. The mathematical difference between the composition of the fossil vegetation of Wiesa and the extant SE Asian vegetation units is 14.19 %, 16.36 % and 17.20 %, respectively. Other, less similar units are situated in Europe and Japan.

The Taxonomic Similarity Drudge 1 and 2 tool reveals an approximately 25 % similarity to units in E and SE Asia, namely “Mixed Mesophytic Forest – Tianmu-Shan (Zhejiang)”, “Broad-leaved Deciduous Forest (Eastern Guizhou)”, “Mixed Mesophytic Forest – Southern Anhui”, and two units on Mt. Fuji, Japan. The Result-Mix Drudge 1 and Result-Mix Drudge 2 tools point to the same several E and SE Asian vegetation units; however, they are listed in different orders for the two result mixes. Hence, the fossil vegetation of Wiesa is most comparable to “Broad-leaved Evergreen Sclerophyllous Forest (Southern Hunan)” in the Result-Mix Drudge 1 results and to “Broad-leaved

Table 1. Phytogeographical context of nearest living relatives or ecological equivalents of 120 fossil-taxa from late Early Miocene Wiesa assemblage in eastern Germany, summarized from Appendix II; *nearest living relative/ecological equivalent distributed on both hemispheres.

Geographic distribution of nearest living relative and/or most similar extant taxon	# of fossil-taxa	Remarks on fossil-taxa
E/SE Asia	55	for individual species relationships of these taxa see Table 2
Disjunction N America – E/SE Asia (ASA)	3	fossil-species of genera *Symplocos*, *Torreya*, *Trema*; relationships to either N American or E/SE Asian species not determinable
N America	13	fossil-species of cosmopolitan genera (3 spp.), N American endemic genus (*Decodon*), 6 genera with ASA disjunction (8 spp.)
Mediterranean	3	fossil-species of Northern Hemisphere genera *Abies* (1 sp.) and *Liquidambar* (1 sp.), and endemic European/N African genus *Tetraclinis* (1 sp.)
Macaronesia	2	fossil species of endemic genus *Visnea* (1 sp.), cosmopolitan genus *Ilex* (1 sp.)
Northern Hemisphere	4	fossil-species of *Frangula* (1), *Nuphar* (1), *Scirpus* (1), *Vitis* (1)
Southern Hemisphere	2	fossil-species of almost cosmopolitan genus *Myrica* (1), Paleotropis/Neotropis genus *Passiflora* (1)
Cosmopolitan*	6	fossil-species of *Aldrovanda*, *Brasenia*, *Dioscorea*, *Ficus*, *Rubus*, *Selaginella*
Extinct	8	fossil-genera of Araceae (2), Malvaceae (1), Mastixioideae (3), Pinaceae (1), Symplocaceae (1)
Not applicable	24	systematic relationships of fossil-taxa not clear

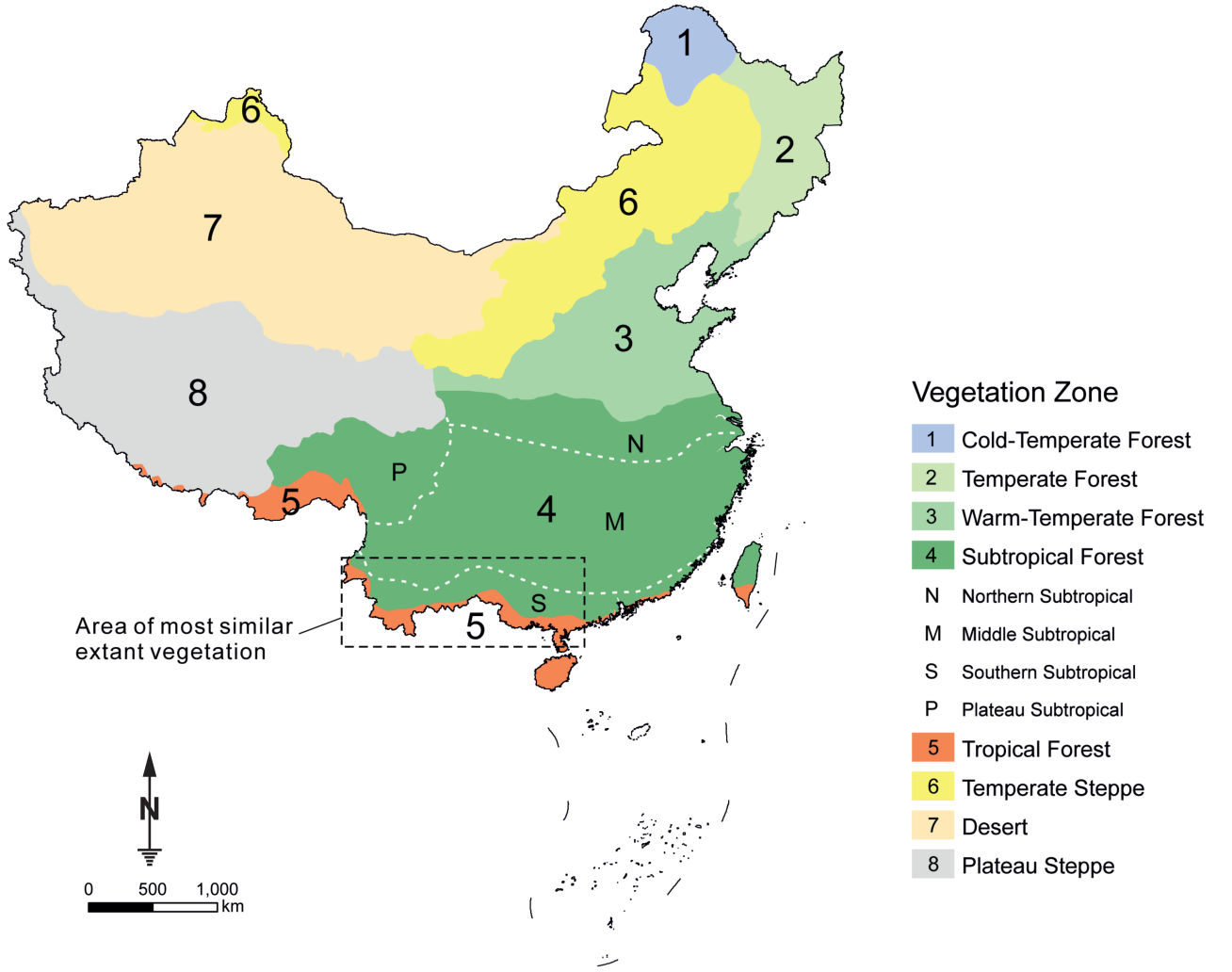

Text-fig. 5. Vegetation zones in P. R. China (Editorial Committee of Vegetation Map of China, The Chinese Academy of Sciences 2007), and assumed location of extant reference vegetation type of Wiesa fossil assemblage (rectangle), as revealed from qualitative floristic analysis. Extant reference vegetation type present in southern belt of zone of subtropical evergreen broadleaved forest, with minor overlap into zone of tropical forest.

Table 2. List of fossil-taxa of late Early Miocene Wiesa assemblage in East Germany, with nearest living relatives or ecological equivalents having (partly) E/SE Asian distribution areas, extracted from Appendix II; compiled and revised from Mai 1999a, b, 2000a, b, Kunzmann and Mai 2005, Mai and Martinetto 2006, Kunzmann 2014; extant taxa with asterisk used for PRRA analysis.

Family / fossil species	Nearest living relative or ecological equivalent taxon in E/SE Asia
Pinaceae	
Cathaya bergeri / *C. roseltii*	*C. argyrophylla**
Keteleeria hoehnei	*K. davidiana**
Nothotsuga protogaea	*N. longibracteata**
Pinus grossana	*P. wallichiana**
Pinus hampeana	*P. massoniana**
Pseudolarix schmidtgenii	*P. amabilis**
Pseudotsuga jechorekiae	*P. sinensis**
Tsuga schmidtiana / *T. schneideriana*	*T. dumosa** / *T. sinensis*
Cupressaceae	
Quasisequoia couttsiae	*G. pensilis**
Taxaceae	
Taxus engelhardtii	*T. mairei**
Ginkgoaceae	
Ginkgo adiantoides	*Ginkgo biloba**
Magnoliaceae	
Liriodendron geminata	*L. chinensis**
Lauraceae	
Cinnamomum costatum	*C.* section *Camphora*
Palmae	
Calamus daemonorops	*C.* spp.*
Pontederiaceae	
Monochoria striatella	*M. plantaginea*
Menispermaceae	
Sinomenium cantalense	*S. acutum**
Sabiaceae	
Meliosma wetteraviensis	*M. veitchorum**, *M. alba*
Hamamelidaceae	
Corylopsis longehilata	*C.* spp.*
Distylium fergussonii	*D. racemosum**
Fortunearia europaea	*F. sinensis**
Vitaceae	
Ampelopsis malvaeformis	*A. delavayana**, *A. leeoides*
Parthenocissus britannica	*P. henryana**, *P. thompsonii*
Tetrastigma chandleri	*T.* spp. (*T. lanceolarium*)
Tetrastigma lobata	*T.* spp.
Vitis globosa	*V. thunbergii*
Vitis teutonica	*V.* spp.
Rosaceae	
Prunus leporimontana	aff. *P. serrulata*, *P. pseudocerasus*
Prunus pereger	*P. kansuensis**, *P. ferganensis*
Sorbus herzogenrathensis	*S. foliolosa**
Rhamnaceae	
Zizyphus striatus	*Z. incurva**
Cannabaceae	
Gironniera carinata	*G.* spp.
Fagaceae	
Quercus rhenana	
Quercus sp. (folia)	
Trigonobalanopsis exacantha / *T. rhamnoides*	*Trigonobalanus* (*Formanodendron*) *doichangensis**

Table 2. continued

Family / fossil species	Nearest living relative or most similar extant taxon in E/SE Asia
Myricaceae	
Myrica boveyana (= *M. wiesaensis*)	*M. javanica**
Myrica stoppii	*M. nagi*, *M. rubra*
Juglandaceae	
Cyclocarya cyclocarpa	*C. paliurus**
Engelhardia orsbergensis	*E. roxburghiana**
Euphorbiaceae	
Sapium germanicum	*S. sebiferum**
Combretaceae	
Quisqualis pentaptera (?*Craigia bronnii*)	(*Craigia kwangsiensis*)
Staphyleaceae	
Turpinia ettingshausenii	*T. formosana**, *T. tomifera*, *T. montana*
Rutaceae	
Phellodendron lusaticum	*P.* spp.*
Toddalia maii	*T. asiatica**
Malvaceae	
Burretia instructa	(*Craigia* or *Tilia*)
Polygonaceae	
Polygonum leporimontanum	aff. *P.* section *Pleuropterus*
Mastixiaceae (Cornaceae)	
Diplopanax limnophilum	*D. stachyanthus**
Mastixia lusatica	*M.* spp.*
Pentaphylacaceae	
Eurya stigmosa	*E. japonica**
Theaceae	
Polyspora hradekense / *P. europaea*	*P.* spp.*
Symplocaceae	
Symplocos casparyi (*S. lignitarum, S. salzhausensis*)	*S. sulcate** (*macrophylla*), *S. ophirensis*
Symplocos pseudogregaria	*S. anomala**, *S. tingifera*, *S. kuroki*
Symplocos schereri	*S. tankae*, *S. costata**, *S. crassilimba*, *S. cerasifolia*
Sphenotheca incurve	extant Asian *Symplocos* spp.*
Sphenotheca gigantea	extant Asian *Symplocos* spp. *
Styracaceae	
Rehderodendron ehrenbergii	*R.* spp.
Rehderodendron wiesaense	*R. kwangtungense**
Paulowniaceae	
Paulownia cantalensis	*P.* spp.*

Deciduous Forest (Eastern Guizhou)" in the Result-Mix Drudge 2 results. More detailed data for the units and similarity percentage values are available in Appendix IV.

Palaeofloristic comparison

A detailed floristic comparison between the floras of Borna-Ost/Bockwitz TC, Wiesa and Wischgrund is documented in Appendix I. The occurrences of climate-sensitive genera and families forming the forest structures combined with relative abundance data are separately considered (Tab. 5). In particular, we treated Mastixioideae, Fagaceae, Lauraceae and Betulaceae.

Borna-Ost/Bockwitz TC is distinguished from Wiesa by the occurrence of "old" thermophilous elements such as *Eotrigonobalanus furcinervis*, *Platanus neptuni*, and *Majanthemophyllum petiolatum*. Subtropical taxa with long stratigraphical ranges such as *Mastixia amygdalaeformis*, *Quasisequoia couttsiae*, *Sphenotheca minuta*, *Symplocos* spp., and *Trigonobalanopsis rhamnoides* are rare, and palms have not been proven to date. Lauraceae are markedly diverse, including fossil-species of *Daphnogene*, *Laurocarpum*, and *Laurophyllum*. Temperate, mostly deciduous taxa are predominant in this assemblage. These taxa are *Acer* spp., *Alnus rostaniana*, *Carpinus grandis*/*cordataeformis*, *Cyclocarya cyclocarpa*, *Fagus saxonica*/*F. deucalionis*, *Liquidambar europaea*, *Populus* spp., *Ulmus* spp. and *Taxodium dubium*. From Wiesa, only *Alnus* sp., *Liquidambar europaea*, and *Cyclocarya cyclocarpa* are recorded. Borna-Ost/Bockwitz TC is distinct from the other assemblages by the presence and diversity of Araliaceae.

Table 3. Phytogeographic Reference Regions Assessment: 1.5° grid box resolution analysis; taxon list of nearest living relatives of fossil-taxa from late Early Miocene Wiesa assemblage from 1.5° reference region grid box (arrow in map Text-fig. 4a), located in western Yunnan Province, P. R. China and southern Kachin Province, NE Myanmar (east of Myitkyina city), including their geographic coordinates as provided by GBIF.

Family	Genus	Species	Decimallongitude*	Decimallatitude*
Vitaceae	*Ampelopsis*	*A. delavayana*	98.874167	24.791667
Arecaceae	*Calamus*	*C. wuliangshanensis*	97.6794	24.725
		C. henryanus	97.48	25.67
Hamamelidaceae	*Corylopsis*	*C. himalayana*	97.3717	25.8375
Pentaphylacaceae	*Eurya*	*E. japonica*	98.689166	24.58669
Ginkgoaceae	*Ginkgo*	*G. biloba*	98.8	25.83333
Nyssaceae	*Mastixia*	*M. pentandra*	97.68	24.79
Rutaceae	*Phellodendron*	*P. chinense*	98.543884	25.210833
Pinaceae	*Pinus*	*P. wallichiana*	97.97	25.42
Theaceae	*Polyspora*	*P. longicarpa*	98.746109	24.94833
		P. chrysandra	98.451944	24.948611
Symplocaceae	*Symplocos*	spp.	98.734772	24.857555
		S. cochinchinensis	98.768257	24.830948
		S. dryophila	98.628197	25.793135
		S. glumerata	98.759918	24.828781
		S. kuroki	98.615555	25.807695
		S. paniculata	98.709862	25.40239
		S. racemosa	98.873779	24.787663
		S. racemosissima	98.738333	25.457222
		S. sulcata	98.5277	24.8053
		S. sumuntia	98.650833	25.387941
Taxaceae	*Taxus*	*T. chinensis*	98.5	25.416667
Pinaceae	*Tsuga*	*T. dumosa*	98.615556	25.807778
Rhamnaceae	*Ziziphus*	*Z. incurva*	98.666667	25.666667

Distinctiveness of the Wiesa assemblage is displayed by the presence and diversity of subtropical elements. Mastixioideae are present with 5 genera and 6 fossil-species, of which 4 genera are extinct (Tab. 5; Mai 1993); Symplocaceae are recorded by the extant genus *Symplocos* and two extinct genera, including 7 fossil-species. Climatically sensitive subtropical taxa that are not recorded in the other assemblages are: (a) the deciduous element of extant EBF in S China *Rehderodendron* (Styracaceae) with two fossil-species; (b) the palm *Calamus daemonorops* (Araceaceae), (c) the woody vine *Sinomenium cantalense* (Menispermaceae), (d) the evergreen trees *Gironniera carinata* and *Trema lusatica* (Cannabaceae), (e) the evergreen, most likely small tree *Turpinia ettingshausenii* (Staphyleaceae), and (f) the woody climber *Toddalia maii* (Rutaceae). All these fossil-species are accessory elements. Specific temperate families like Betulaceae and Salicaceae are quite rare, with only one fossil-species of Betulaceae and none of Salicaceae.

From the flora of Wischgrund, no Araliaceae and palms have been recorded to date, and specific subtropical elements such as *Polyspora*, *Rehderodendron*, *Toddalia*, and *Turpinia* are also lacking. Mastixioideae (one fossil-species) and Symplocaceae are still recorded but are very rare; only a few specimens were discovered from this site. Lauraceae are still present, containing the deciduous fossil-species *Sassafras ferretianum*, which is absent in both other assemblages. Compared to the older assemblages, the persistence of some warm-temperate deciduous taxa such as *Cercidiphyllum*, *Liquidambar*, *Magnolia*, *Nyssa*, and Hamamelidaceae needs to be highlighted. Other temperate deciduous taxa including *Acer*, *Ulmus* and *Zelkova*, which are absent from Wiesa, are present in Borna-Ost/Bockwitz TC and Wischgrund. Betulaceae are similarly diverse in Borna-Ost/Bockwitz TC and Wischgrund, but the temperate genus *Corylus* only occurs in the latter site.

Fagaceae are dominant elements in every assemblage, but each occurrence in an assemblage is characterized by the abundance of different genera (Tab. 5). *Fagus* is dominant in Borna-Ost/Bockwitz TC and in Wischgrund, but absent from Wiesa. By contrast, subtropical *Trigonobalanopsis rhamnoides* is quite rare in Borna-Ost/Bockwitz TC, but predominant both in the leaf and diaspore component in Wiesa, and absent from Wischgrund. Abundance and diversity of *Quercus* is also markedly distinct. It is present with a single fossil-species in the late Oligocene, with two rare fossil-species in the late Early Miocene. The Wischgrund flora reveals 9 fossil-species or taxonomic units of *Quercus*.

Palaeoclimate reconstructions

Our CA results for the Wiesa site confirm the values of the CA analyses of Mosbrugger et al. (2005) and Teodoridis and Kvaček (2015). MAT is 17–18.5 °C, lower than Mai's

Table 4. Climate-sensitive fossil-species of late Early Miocene Wiesa flora, with relationships to extant SE Asian species, their assumed NLRs, subzone/belt of evergreen broadleaved forest zone in southern and southwestern P. R. China, and tropical forest zone in southern P. R. China and northern Vietnam in which NLRs are mainly distributed.

Fossil-species at site Wiesa	Nearest living relative in E/SE Asia	Modern occurrence in SE Asia (for comparison see Text-fig. 5)
Pinaceae		
Cathaya bergeri / C. *roseltii*	*Cathaya argyrophylla*	middle and southern belts of subtropical zone
Nothotsuga europaea	*Nothotsuga longibracteata*	middle and southern belts of subtropical zone
Tsuga schmidtiana / *T. moenana* / *T. schneideriana*	*Tsuga dumosa* /*T. sinensis*	middle belt of subtropical zone
Magnoliaceae		
Liriodendron geminata	*Liriodendron chinensis*	middle and southern belts of subtropical zone
Palmae		
Calamus daemonorops	*Calamus* spp.	southern belt of subtropical zone to tropical zone
Hamamelidaceae		
Fortunearia europaea	*Fortunearia sinensis*	northern and middle belts of subtropical zone
Cannabaceae		
Gironniera carinata	*Gironniera* spp.	southern belt of subtropical zone to tropical zone
Fagaceae		
Trigonobalanopsis exacantha / *T. rhamnoides*	*Trigonobalanus doichangensis*	southern belt of subtropical zone to tropical zone
Combretaceae		
Quisqualis pentaptera (aff. *Craigia bronnii*)	(*Craigia kwangsiensis*)	middle and southern belts of subtropical zone
Staphyleaceae		
Turpinia ettingshausenii	*T. formosana, T. pomifera, T. montana*	middle and southern belts of subtropical zone to tropical zone
Mastixiaceae (Cornaceae)		
Diplopanax limnophilum	*Diplopanax stachyanthus*	southern belt of subtropical zone
Mastixia lusatica / *M. amygdalaeformis*	*Mastixia* spp.	southern belt of subtropical zone
Theaceae		
Polyspora hradekense / *P. europaea*	*Polyspora* spp.	middle and southern belts of subtropical zone
Styracaceae		
Rehderodendron wiesaense	*Rehderodendron kwangtungense*	middle and southern belts of subtropical zone

(2000b) estimate, i.e., 18–21 °C (Tab. 6). The BA reveals slightly lower MAT: 15.9–16.7 °C. Values for WMMT are fairly consistent above 25 °C in all studies, whereas values for CMMT spread with a minimum temperature of 4 °C (Mai 2000b) and a maximum temperature of 12.3 °C (Teodoridis and Kvaček 2015). The values of CA-based MAP calculations are also consistently above 1,000 mm. The BA calculates slightly higher MAP, and Mai's (2000b) maximum value is 2000 mm. In our study, both CA and BA reveal marked seasonality in precipitation by wetter growing seasons (summer) and drier but not dry winters. The climate type is Cfa (warm temperate, fully humid, hot summers, WMMT > 22 °C) according to the Köppen-Geiger classification (Kottek et al. 2006), or Cf (subtropical, no dry season, MPDry > 30 mm) according to the Köppen-Trewartha classification (Belda et al. 2014; Tab. 9).

Applying IA (Mai 1995) and ODA (Yang et al. 2007) to the result of the PRRA, we obtained climate parameters for two places within the area of the 1.5° reference region grid box (Text-fig. 4a: arrow) provided by Climate-Data.org (2021). (1) Tenchong city (western Yunnan, P. R. China; 1,673 m a.s.l.): the regional climate type is Cwb, according to Köppen-Geiger, with MAT 15.3 °C, CMMT 9.5 °C (T_{min} 2.2 °C), WMMT 19.3 °C, MAP 1,940 mm, January precipitation 23 mm, July precipitation 466 mm. (2) Myitkyina (Myanmar, 145 m a.s.l.), located at the northeastern margin of the grid box area: the regional climate type is Cwa, according to Köppen-Geiger, with MAT 23.0 °C, CMMT 16.7 and WMMT 26.2 °C; compared to Tenchong, precipitation is slightly higher and precipitation seasonality is slightly more distinct.

Focusing on the major extant reference vegetation types, namely (a) the southern belt of subtropical evergreen broadleaved forest and its transitions into the tropical forest biome, and (b) the tropical mountain evergreen broadleaved forests in higher elevations in SW and S China (Text-fig. 5), the following Köppen-Geiger climate types are deduced from the maps in Peel et al. (2007): (1) warm-oceanic type (Cfa), (2) subtropical humid type (Cwa), and (3) subtropical oceanic type in highlands (Cwb) as present in higher elevations in Yunnan. The Köppen-Trewartha classification system covers the complete zone of evergreen broadleaved forest and the transitional zone to the tropical forest in SE Asia by the Cf zone (subtropical climate + no dry season; Belda et al. 2014).

The calculation of mean month temperatures using the equation of Grein et al. (2013) reveals for the Wiesa site that only one month has MMT clearly below 10 °C, two months show MMT of 9.9 °C (Tab. 7). This means that the growing season length is about 11 months – almost the entire year.

Table 5. Occurrences and relative abundances of genera and fossil-genera of Mastixioideae (Nyssaceae), Fagaceae, Lauraceae and Betulaceae in three study assemblages in central and eastern Germany. [2] based on Mai and Walther 1991 with updates by Moraweck et al. 2019; [3] based on Mai 1999b, 2000a, b with updates by Kunzmann and Mai 2005, Mai and Martinetto 2006, Kunzmann 2014; [4] based on Striegler 2017.

Fossil-genus[1] / genus	late Oligocene Borna-Ost/Bockwitz TC[2]	late Early Miocene Wiesa[3]	Late Miocene Wischgrund[4]
Mastixioideae			
Diplopanax			
Eomastixia[1]			
Mastixia			
Retinomastixia[1]			
Tectocarya[1]			
Fagaceae			
Castanea			
Eotrigonobalanus[1]			
Fagus			
Quercus			
Trigonobalanopsis[1]			
Lauraceae			
Cinnamomum			
Daphnogene[1]			
Laurinoxylon[1]			
Laurocarpum[1]			
Laurophyllum[1]			
Ocotea			
Sassafras			
Betulaceae			
Alnus			
Betula			
Carpinus			
Corylus			

	No record
	1–10 records (rare)
	10 – 100 records (abundant)
	>100 records (very frequent)

The Borna-Ost/Bockwitz TC and Wischgrund sites have shorter growing seasons, at 9 months (Tab. 7). Therefore, the climate type by the classification of Köppen-Trewartha (Belda et al. 2014) for both sites is constantly Cf, because 8–12 months have a MMT > 10 °C.

Based on Striegler's (2017) revision of the macroflora of Wischgrund (87 taxa), our CA analysis provides the following results (Tab. 8): MAT ranges between 15.7 and 16.5 °C; WMMT is 25.7–26.4 °C, with NLR *Nyssa sinensis* as warm outlier and NLRs *Fraxinus excelsior* and *Betula subpubescens* as cold outliers; CMMT is 3.6–4.8 °C, with Mastixioideae as outliers; MAP estimate reveals 1,096–1,153 mm/a. The analysis also revealed seasonality in precipitation. Precipitation of the wettest month is 164–185 mm, while 25–32 mm is calculated for the driest month. Precipitation values for the warmest month of 132–141 mm indicate wet summers and growing seasons and drier winters.

Discussion

Phytogeographic Reference Region Assessment

The results show that only the 1.5° and 2° grid resolutions provide proper and indicative data. The 3° resolution yields some medium-high co-occurrence values, but defines a rather large zone of extant reference vegetation. Interestingly, this large zone is a latitudinal area. Higher grid resolution (1°) significantly lowers the co-occurrence values. The low co-occurrence values per grid box could

Table 6. Reconstruction of palaeoclimatic parameters for late Early Miocene Wiesa fossil flora, eastern Germany: comparison of new results with published data; CA – Coexistence Approach; BA – Bioclimatic Analysis; [1] classification of Köppen-Geiger (Kottek et al. 2006); [2] classification of Köppen-Trewartha (Belda et al. 2014); [3] taxa are same as for PRRA (Tab. 2); [4] taxa of 1.5° reference region grid box listed in Table 3.

Reference	#taxa	Climate type	MAT [°C]	CMMT [°C]	WMMT [°C]	MAP [mm]	MPWet [mm]	MPDry [mm]
Mai (2000b)	>100	Cfa[1], warm temperate, humid	**18–21**	**4–10**	**25–28**	**800–2,000**	–	–
Mosbrugger et al. (2005): CA	89		**17.5-18**	**9.6**	**26.5**	**1,146–1,355**	–	–
Teodoridis and Kvaček (2015): CA	(?)	subtropical	**17.2–18.0**	**7.7–12.3**	**26.5–28.2**	**1,246–1,355**	–	–
CA (this study)	86	Cfa[1] Cf[2]	**17–18.5**	**7.7–9.6**	**26.5–26.9**	**1,194**	**182–195**	**37–43**
BA (this study)	17[3]	Cfa[1] Cf[2]	**15.9–16.7**	**6.3–6.4**	**25.0–26.7**	**1,428–1,535**	**259–286**	**36–38.5**

Table 7. Reconstruction of palaeoclimatic parameters: mean month temperatures (MMT, calculated by equation from Grein et al. 2013) and growing season length (GSL: all months with MMT > 10 °C); MAT: value of half distance between MAT_{min} and MAT_{max} from CA. Sources for CA values: Borna-Ost/Bockwitz TC (BOB TC) – Moraweck et al. 2019; Wiesa and Wischgrund – this study.

	MMT [°C]													
Month / Site	J	F	M	A	M	J	J	A	S	O	N	D	GSL	MAT [°C]
Wischgrund	5.2	6.7	10.7	16.1	21.6	25.5	26.9	25.5	21.6	16.1	10.7	6.7	**9**	16.1
Wiesa	8.7	9.9	13.2	17.7	22.3	25.6	26.8	25.6	22.3	17.7	13.2	9.9	**(9)–11**	17.75
BOB-TC	6.0	7.3	10.9	15.9	20.9	24.5	25.8	24.5	20.9	15.9	10.9	7.3	**9**	15.9

Table 8. Comparison of qualitatively and quantitatively estimated palaeoclimate parameter values for central and eastern German sites Borna-Ost/Bockwitz TC (late Oligocene), Wiesa (late Early Miocene) and Wischgrund (Late Miocene); [1] for Tenchong, western Yunnan, P. R. China; [2] for Myitkyina, Myanmar; for abbreviation of approaches see Methodology and methods.

Site (reference)	Approach	MAT [°C]	CMMT [°C]	WMMT [°C]	MAP [mm]	Remark
Borna-Ost/ Bockwitz TC (Moraweck et al. 2019)	CA	**15.7–16.1**	**5.0–6.2**	**25.4–25.6**	**1,231–1,355**	–
	CLAMP	**10.1** (±1.3)	**–1.8** (±2.6)	**22.6** (±1.7)	**(GSP) 878.4** (±497)	–
Wiesa (this study)	CA	**17–18.5**	**7.7–9.6**	**26.5–26.9**	**1,194**	–
	BA	**15.9–16.7**	**6.3–6.4**	**25.0–26.7**	**1,428–1,535**	–
	IA / ODA[1]	**15.3**	**9.5**	**19.3**	**1,940**	T_{min}: 2.2 °C
	IA / ODA[2]	**23.0**	**16.7**	**26.2**	**2,345**	–
Schipkau Floristic Complex (incl. Wischgrund) (Mai 2001b)	argumentatively	**13–15**	**–2.5–1.0**	**20–27**	**500–1,300**	regularly frosts and absolute minimum –5.5 °C
Klettwitz-12 (Wischgrund) (Teodoridis and Kvaček 2015)	CA	**15.7–16.3**	**4.7–6.2**	**25.7**	**979–1,355**	–
Wischgrund (this study)	CA	**15.7–16.5**	**3.6–4.8**	**25.7–26.4**	**1,096–1,153**	–

be an effect of detailed heterogeneity of the vegetation, but may also indicate that native vegetation is only sparsely distributed in the subtropical and tropical zones in SE Asia, due to thousands of years of anthropogenic influences. In the analysis with the most useful grid resolution of 1.5°, almost all grid positions with co-occurrences of more than three genera of the NLRs are plotted within the central and southern Chinese zone of EBF, but highest co-occurrence values are present in the southern part of the subtropical belt (Text-fig. 5). The highest co-occurrence values (colored red in Text-fig. 4) are in southwest and central-southern China (Yunnan, Guangxi, Hunan, Hubei, Jiangxi and Guangdong provinces) and on Taiwan Island. However, because GBIF data are not equally collected from each region, Taiwan may contribute more data to the co-occurrence values than other regions. Therefore, the high values on this island should be treated with caution (Meyer et al. 2016), and they are excluded from our analysis.

The area of the extant reference vegetation encompasses several distribution areas of extant relics, such as *Cathaya argyrophylla* and *Nothotsuga longibracteata*. It must be noted that relic areas are often additionally reduced by anthropogenic activities (culture, agriculture), and do not necessarily represent the full ecological capacity of the taxon (e.g., *Metasequoia*; Wang et al. 2019). Hypothetically, some co-occurrence values of grid boxes are potentially even higher, considering a prehistorically wider distribution of relics.

As already mentioned, extant subtropical EBF in central and south China is not homogenous, but varies in composition and key elements, depending on (i) geographical latitude and longitude, (ii) distances from the ocean and therefore amount of monsoonal influence, (iii) topographical factors (relief, mountains), and (iv) geological underground. Based on these preconditions, the extant distribution area of subtropical forests in E and SE Asia is subdivided into several specific subunits; the coarsest subdivision provides three belts that are generally correlated with geographical latitude (Text-fig. 5); a fourth belt represents the SE Tibetan Plateau and the Hengduan Mountains (Text-fig. 5). Only the border between the northern and the middle belt does not exclusively follow circles of latitude. For the Wiesa assemblage, critical taxa among NLRs that are quite sensitive vegetation and climate proxies (Tab. 4) are indicative for the transition from the middle to the southern subtropical EBF belt, the southern subtropical belt and the transition from the southern subtropical EBF to the tropical forest belt.

Some important climate-sensitive species, such as *Mastixia* spp., *Diplopanax stachyanthus*, and *Trigonobalanus* (*Formanodendron*) *doichangensis*, are in fact species of the tropical-subtropical transition zone that are not strictly distributed in subtropical East Asia, but do occur in tropical Asia. Moreover, the coexistence of these taxa would in fact predict that the most similar forest of the fossil Wiesa assemblage is a tropical mountain evergreen broadleaved forest transitioning from a tropical to a subtropical zone. Other climate-sensitive species of the NLRs have distribution areas that are extended to the equatorial regions of Australasia (Text-fig. 4). However, these species mostly occur in mountain regions that provide subtropical conditions instead of tropical ones at certain elevations. Such species are, for instance, *Engelhardia roxburghiana* in Borneo (Indonesia) and *Polyspora* spp. in Vietnam, Laos and northern Indonesia. In contrast to the climate-sensitive species mentioned above, these tropical mountain elements do not co-occur, and thus these areas, e.g., central and southern Vietnam, revealed lower co-occurrence values (Text-fig. 4).

All other taxa listed in Tab. 2 are less climate-sensitive, which means that their distribution area covers all vegetation belts of the area of subtropical forest and even beyond.

Additional genera might also be regarded as sensitive proxies for the selection of the extant reference vegetation for the Wiesa assemblage, but it is not clear if the extant NLRs come from E/SE Asia or from elsewhere. These genera are *Leucothoe*, *Passiflora*, and *Trema*. If their NLRs come from E/SE Asia, they would be also indicative for the middle and southern EBF belts of the subtropical zone and the transition to the tropical zone. Additional concern comes from *Sequoia*, which was present in central and southern China until the Neogene (Zhang et al. 2015). There, *Sequoia maguanensis* is assumed to be an indicator for "weak monsoon", and its disappearance during the Neogene (Late Miocene) is related to the firm establishment of the dry winter season in the monsoonal areas (Zhang et al. 2015).

Comparison PRRA and IPR results

As expected, the basic IPR Vegetation Analysis (Kovar-Eder and Kvaček 2007, Kovar-Eder et al. 2008, Teodoridis et al. 2011) revealed EBF as the major zonal vegetation type for the Wiesa assemblage, although the revision and update of the taxon list compared to Mai's (2000b) list produced some adjustments in the interpretation of NLRs and ecological equivalents (EEs). Proposals of NLRs for *Symplocos* species sensu Mai and Martinetto (2006) and proposals for NLRs for extinct *Sphenotheca* sensu Manchester and Fritsch (2014) are such updates (App. II). The percentage of BLE within the zonal woody angiosperm component is consistently between 45 % and 46 %, which is clearly above the threshold of 40 % for the BLE component within the EBF vegetation type (Teodoridis et al. 2011), so our result coincides with the earlier analysis of Teodoridis and Kvaček (2015). There is additional room for interpretation for the assignment of some fossil-taxa from Wiesa to the taxonomic-physiognomic groups of IPR, e.g., if the *Nyssa* species are exclusively azonal woody components or if they should be scored as being 50 % azonal woody and 50 % zonal components. The same is the case for *Alnus* sp., *Cyclocarya cyclocarpa*, "*Illicium*" *germanicum* and *Quercus* sp. Anyway, the percentages of BLD and BLE differ only by a minor amount – less than 1 %.

There is no threshold for an ecotone between EBF and tropical forest, or for tropical forest in the IPR scheme for identifying zonal vegetation types (Teodoridis et al. 2011). The reason could be that clear tropical vegetation is not expected in European mid-latitude late Paleogene and Neogene assemblages, which was already assumed by Mai (1995) for the complete Cenozoic in northern central Europe. Even the Messel assemblage in western Germany, originating from the EECO, is attributed to "quasiparatropical" palaeovegetation (Kvaček 2010). However, we evaluate here the climatic sensitivity of some fossil-taxa of Wiesa as being relatives of extant taxa with a transitional subtropical-tropical climatic preference (Tab. 4). Our PRRA points towards an EBF type and its transition to tropical montane evergreen forest as most similar vegetation type. The two approaches show differences in the results for the major zonal vegetation type.

A similar difference in the results of the PRRA and IPR approaches is stated when comparing both the vegetation of the reference grid boxes and the extant vegetation of the major reference region (Text-fig. 5) against the estimates of the most similar extant vegetation revealed from the Drudge 1 and 2 tools. Beside various vegetation types outside SE Asia (e.g., in the Caucasus region and in Japan) and the "Montane Coniferous Forest – Taiwan" (App. IV), the results of the IPR Similarity Approach point to "Broad-leaved Evergreen Sclerophyllous Forest (Guizhou)" and "Broad-leaved Evergreen Sclerophyllous Forest – Pine

Forest (Yunnan)" as most comparable extant units, instead of a transition between EBF and tropical montane evergreen forest in our PRRA result. However, the extant vegetation units from the IPR Similarity Analysis are also situated in the southern belt of the EBF in southern P. R. China. There is a marked overlap between the Similarity Analysis results from Drudge 1 and 2 tools, meaning that the inclusion of zonal herbs in the Drudge 2 tool does not significantly change the results.

For Taxonomic Similarity, the IPR approach reveals several vegetation units of mixed mesophytic forest and broad-leaved deciduous forest (App. IV), but no unit of EBF. These units are consistently less subtropical than the vegetation of the reference vegetation estimated in our PRRA. The IPR Taxonomic Similarity approach refers to vegetation units that seemingly underestimate the role of subtropical/tropical elements in the Wiesa flora. These elements are exclusively woody angiosperms, except for *Calamus daemonorops* (palms). Interestingly, the Results-Mix Drudge 1 tool better meets the results of the Similarity Analysis in revealing "Broad-leaved Evergreen Sclerophyllous Forest (Southern Hunan)" as most similar unit; by contrast, Results-Mix Drudge 2 tool refers to more temperate vegetation, i.e., "Broad-leaved Deciduous Forest (Eastern Guizhou)".

Both PRRA and the IPR approaches have the same goals, which is estimating the most similar vegetation type for a fossil assemblage and where this vegetation type occurs. In general, both methodologies clearly refer to E and SE Asian flora as the most similar extant vegetation and taxonomically most similar units for the fossil flora of Wiesa, which is in accordance with all previous interpretations. But both methodologies are based on quite different approaches, and when looking into details, their results for Wiesa differ in our study. IPR utilizes similarities in the proportions of zonal key elements of fossil assemblages and a calibration dataset of differently-sized modern vegetation units from Eurasia, ranging from a single mountain to larger areas of Chinese provinces (Teodoridis el al. 2020); PRRA reconstructs a reference region with maximum overlapping of the distribution areas of NLRs/EEs, and the reference region contains the extant reference vegetation type. The area of the reference region is thus defined by the size of the overlapping area, and not by the size of an area of a particular calibration dataset. Reference regions could also include areas for which no detailed vegetation data acquisitions exist as taxon lists, which is why such areas cannot be part of the calibration dataset of IPR Similarity Approach. On the other hand, PRRA relies on quality and quantity of phytochorological data in GBIF, which are indeed heterogeneous, as mentioned above. It is a disadvantage for PRRA that not all phytochorological data on GBIF have the same quality level that eventually reduces the maximum number of NLRs in grid boxes when running analyses. Theoretically, PRRA can be applied to every Cenozoic flora worldwide, but the quality of results mainly dependents on the quality and quantity of GBIF data. Quality and quantity of calibration datasets are the limitations of the IPR Similarity Analysis, which is currently based on a dataset encompassing 505 Eurasian floristic types (Teodoridis et al. 2020). This dataset is necessarily partly a random compilation, because it relies on what has been published. In any case, the backbones of both approaches are co-occurrences of extant taxa (IPR – zonal key genera; PRRA – all genera) and autecological interpretations of fossil and extant taxa. Basically, they rely on the excellence of taxonomic determinations of fossil plants in a flora, and are only applicable if a fossil flora is appropriately well-studied. Additionally, IPR Vegetation Analysis and Similarity Approach depends on the physiognomic interpretation of fossil-taxa. Except for the basic IPR Vegetation Analysis, which was introduced in 2003 (Kovar-Eder and Kvaček 2003, Kovar-Eder et al. 2008, Teodoridis et al. 2011), both similarity approaches are newly introduced routines, which will probably need adjustments in the future.

Remarks on palaeofloristic aspects

Vomela (2016) used palynological investigations to confirm the palaeoecological and palaeophytosociological interpretations of the Wiesa flora, based on macro-fossils identified by Mai (2000b). As usual in the fossil record, the palynoflora is more diverse than the macroflora. However, some key taxa for palaeovegetational and palaeoclimatic reconstructions show similar occurrence/absence signals in both assemblages, e.g., Betulaceae are only present with *Alnus*, and Fagaceae are recorded by *Trigonobalanopsis* and *Quercus*. The latter is present by several distinct pollen morphotypes, while only a single taxon based on seeds and a single taxon based on leaves are known from the macro-fossil record (App. I). By contrast, some climate-sensitive taxa of the macroflora that are indicative for subtropical to tropical climate are not proven from the palynoflora, e.g., *Quisqualis pentaptera* (aff. *Craigia*), *Gironniera carinata* and *Turpinia ettingshausenii*. Pollen taxa indicating tropical-subtropical climate that are not present in the macroflora are Sapotaceae div. sp. and Cyrillaceae indet. (Vomela 2016). It must be noted that Vomela's (2016) study is only a preliminary investigation of palynomorphs from the Wiesa section, because it was conducted on a single study sample of unknown lithostratigraphic position.

Interestingly, *Fagus* is also absent from the palyno-assemblage. Additional valuable hints on the presence and/or absence of *Fagus* in the region come from the Early-Middle Miocene floras of Hrádek nad Nisou in the Czech Republic (Holý et al. 2012). In Hrádek, *Fagus* appears relatively late in the section, after those levels that bear comparable floras to the Wiesa assemblage. Therefore, it can be argued that the broadleaved deciduous element *Fagus* was indeed absent during the subtropical conditions in the late Early Miocene.

The analysis of the three regional fossil floras by occurrence/absence data and relative abundances of climate-sensitive genera and families demonstrates that the flora of Wiesa and Wischgrund are markedly distinct. While Wiesa shows the high abundance and diversity of subtropical elements and the predominance of subtropical indicators such as Mastixioideae, Symplocaceae and *Trigonobalanopsis*, only a few thermophilic elements are recorded in Wischgrund, such as the only mastixioid *Eomastixia saxonica* (Striegler 2017). Moreover, presence/absence and abundancy data of genera of the temperate family Betulaceae indicate similar distinctiveness (Tab. 5).

Low diversity in Wiesa, i.e., the presence of *Alnus*, is directly opposite to the diversity and abundance in Wischgrund (Tab. 5). In short, as the flora of Wiesa is a proper example for regional palaeovegetation corresponding to the beginning of MCO, Wischgrund is regarded as typical example for regional palaeovegetation indicating the global cooling during the Late Miocene.

Borna-Ost/Bockwitz TC is less distinct from Wiesa, because it encompasses more subtropical and thermophilous taxa compared to Wischgrund, in particular "old" elements such as *Eotrigonobalanus furcinervis*, *Platanus neptuni* and *Majanthemophyllum petiolatum* are present. Both assemblages are also characterized by the diversity and abundance of Lauraceae. In the case of Borna-Ost/Bockwitz TC, it is typical for Oligocene mixed mesophytic forest type floras in northern central Europe (Kvaček and Walther 2001).

Palaeoclimatic estimates

The palaeoclimate assumed for the Wiesa site, based on CA and BA estimates (Tab. 6), is of the Cfa type according to Köppen-Geiger (Kottek et al. 2006) and the Cf type according to Köppen-Trewartha (Belda et al. 2014). The latter climate type is also indicated for the area of the major extant reference vegetation type; however, this reference area covers more than one climate type in the Köppen-Geiger system; besides Cfa, it also includes Cwa and Cwb. Evaluating the results from IA/ODA for climate classification within the area of the 1.5° reference region grid box, Cwa and Cwb types are deduced, but not Cfa. These are quite remarkable results. While the Cfa type means that precipitation is more evenly distributed through the year, the Cwa/b types indicate a winter drought like in SE China, with monsoon-like or summer-monsoonal climate. Medium to high MAP values, i.e., 800–2,000 mm, and seasonality in precipitation have been already deduced by Mai (2000b), which mirrors the intensity of SE Asian monsoon in the distribution area of extant EBF. However, based on the actualistic perspective, Mai (2000b) concluded a seasonal climate, but did not assume monsoon-like conditions. Monsoon-like seasonality in precipitation is not likely for central Europe during the Early-Middle Miocene, because the study area was situated in the same palaeolatitude as today (appr. 51° N), which implies a location in the area of the westerlies. In CA and BA, precipitation seasonality is consistently estimated with wet summers and drier but not dry winters. This seasonality signal comes partly from NLRs distributed in monsoonal regions of E and SE Asia. However, leaf physiognomy-based CLAMP results for Early and Middle Miocene floras from the northern Czech Republic, such as the Kristina Mine flora (Zittau Basin, Czech Republic) and the Horní Bříza flora (Plzeň Basin, Czech Republic) also revealed a distinct seasonality of precipitation (Holý et al. 2012, Teodoridis and Kvaček 2015). For the latter flora, seasonality in precipitation is also assumed from the results of an IPR Vegetation Analysis (Kovar-Eder and Teodoridis 2018). It remains an open question if the Cwa/b interpretation from the IA/ODA analysis could indeed mirror a slightly different palaeoclimate for the eastern German region during the late Early Miocene, compared to many other estimations from the Early and Middle Miocene of that region revealing Cfa climate (e.g., Utescher et al. 2009), or if these results are markedly biased by the higher impact of NLR proxies in this approach. The former would imply that the IA/ODA approach could be more sensitive in palaeoclimate estimation. The latter would demonstrate that NLRs and the maximum overlap distribution area of NLRs are not necessarily in any case proper climate proxies. Consequently, PRRA would deliver a most similar vegetation unit that is growing under climate conditions somehow dissimilar from the estimated palaeoclimate conditions at the fossil site, at least regarding precipitation. However, the degree of seasonality in precipitation in our CA and BA results is pronounced. The threshold for Cw climate against Cf climate is given by Kottek et al. (2006) as follows: value for maximum summer precipitation more than 10 times as much as the value for minimum winter precipitation, and minimum summer precipitation value exceeds minimum winter precipitation value. In our values, maximum summer precipitation is 5.3 times (CA)/7.9 times (BA) as much as the minimum winter precipitation. At least the estimates from BA are close to the threshold, which leads to the conclusion that the palaeoclimate type at site Wiesa could have been transitional between Cf and Cw.

Until today, no non-plant-based palaeoclimate calculations are available for the Wiesa site. The absence of any hard parts (skeleton, teeth) of animals in the sediments does not allow for isotope-based calculations. Therefore, it is currently impossible to conclusively assess the reliability of our palaeoclimate estimates for Wiesa. Until other estimates become available, the plant-based values should be treated with caution – at least the values indicating the degree of seasonality in precipitation.

Another interesting result is that the observed differences in the composition of the three study assemblages constantly reveal the same climate, based on the CA-derived estimates in both climate classification systems (Tab. 8). These types are the Cf type according to Köppen-Trewartha and Cfa type according to Köppen-Geiger (Tab. 8). The dominance of the Cfa climate type throughout most of the Oligocene and until the Late Miocene was also revealed in a detailed study on present-day climatic equivalents of European Cenozoic climates, conducted on palaeobotanical sites of the Cenozoic North Sea realm (Utescher et al. 2009).

Looking into details, CA values for the Borna-Ost/Bockwitz TC and Wischgrund sites show no significant differences in MAT and WMMT, compared to values for Wiesa (Tab. 8). The calculations for the late Oligocene site reveal MAT of about 16 °C and WMMT of about 25 °C. The CA-based MAT estimates for Wiesa (i.e., 17–18.5 °C) apparently point to somewhat warmer conditions towards the beginning of MCO. Somewhat cooler conditions with MAT 15.5–16.5 °C are calculated for the Late Miocene site, which coincides in time with the gradual global cooling. Analogously, CMMT values show cooler conditions in the late Oligocene (Borna-Ost/Bockwitz TC: 5–6 °C) and in the Late Miocene (Wischgrund: 5–6 °C), compared to the values derived from Wiesa (~8–11 °C). However, CMMTs are still distinctly above 0 °C. A similar decrease in CMMT of the order of 3–5 °C between the Middle and Late Miocene is estimated for regions in western Germany, resulting from

CA analysis of macrofloras of the Rhenish Main Seam, Lower Rhenish Embayment (Utescher et al. 2009).

Some CLAMP estimates markedly differ from CA and BA estimates (Tab. 8). CLAMP results for Borna-Ost/Bockwitz TC (Moraweck et al. 2019) refer to CMMT slightly below 0 °C, while WMMT is 22.6 °C. The differences between CA and CLAMP estimates for Borna-Ost/Bockwitz TC have been explained as "riparian effect" by Teodoridis (2004), because in such parautochthonous fluvial assemblages, leaves of broadleaved deciduous taxa are predominant, and so CLAMP tentatively tends to show cooler temperatures.

Interestingly, Mai (2001b) indicated markedly different palaeoclimate parameters for Wischgrund and coeval sites within the Schipkau Floristic Complex. Using the deductive method, namely using palaeoclimate parameters from a meteorological station in the area of the most similar extant vegetation type, Mai (2001b) settled on palaeoclimate values for the entire Schipkau floristic complex (Text-fig. 3), which includes the Wischgrund site, as follows: significantly colder CMMT (–2.5–1.0 °C) compared to CA values, while MAT and WMMT are rather similar (Tab. 10). In this case, Mai's (2001b) cooler winter temperatures come from his comparison of Wischgrund and other coeval assemblages with extant temperate broadleaved deciduous forests in northern central Europe. Following Mai (2001b), the climate type according to the classification of Köppen-Trewartha (Belda et al. 2014) would be Do or Dc, meaning 4–7 months with MMT > 10 °C and CMMT > 0 °C or < 0 °C, respectively.

Moreover, shorter-term variability of climate and related vegetation changes may cause apparent inconsistencies in the reconstructions, especially when regarding floristic complexes or assemblages combining various fossil-bearing levels. Combined plant records may level out climate-induced signals such as phases, in which a cooler vegetation type may have existed, as was assumed by Mai (1995). Studies on higher resolving micro- and macrofloristic records of the southern North Sea and Lower Rhenish basins point to such short-term changes of climate and vegetation throughout the studied timespan, which can be partly tied to isotope events known from marine strata (e.g., Larsson et al. 2011, Utescher et al. 2012, 2021).

Another remarkable difference between the palaeoclimate estimates for all sites is growing season length, which is longest in Wiesa (about 11 months; Tab. 7). Pre- and post-MCO growing season lengths are markedly shorter, at 9 months (Tab. 7). Which estimations or calculations better reflect regional CMMT before and after MCO will remain uncertain until other approaches produce plant-independent proxies.

Conclusions

The new approach Phytogeographical Reference Region Assessment (PRRA) is introduced to ascertain the area of most similar extant vegetation for the Wiesa macrofloristic assemblage, based on NLRs or EE of fossil-taxa. This area, called a reference region, is situated within the southern belt of subtropical evergreen broadleaved forest in SW and central southern China, and its transitions into the tropical forest biome. Moreover, climate-sensitive tropical-subtropical NLRs point to high similarity with tropical mountain evergreen broadleaved forests in higher elevations in SW China (western Yunnan).

Results of IPR Vegetation Analysis and Similarity approaches, which were conducted for comparison, are in general agreement with respect to the overall relationship of the fossil flora to E and SE Asian subtropical vegetation. However, results for the IPR Similarity and Taxonomic Similarity partly differ from PRRA results in the appraisal of subtropical-tropical taxa for the estimation of most similar extent vegetation units.

Regional floristic comparisons with the pre-MCO flora of Borna-Ost/Bockwitz TC and the post-MCO flora of Wischgrund demonstrate the distinctiveness of the Wiesa flora by the diversity and abundances of subtropical Mastixioideae, Symplocaceae and Lauraceae, and by the presence of climate-sensitive subtropical-tropical taxa such as *Calamus daemonorops*, *Gironniera carinata*, *Rehderodendron* spp., *Sinomenium cantalense*, *Trema lusatica* and *Turpinia ettingshausenii*.

The palaeoclimate at the Wiesa site is characterized as being subtropical and humid, according to the Köppen-Trewartha classification system, with MAT approx. 18 °C or slightly lower, WMMT above 25 °C, and CMMT between 7–9 °C. The growing season during the beginning of MCO lasted almost all year. These mild winters, indicated by an increase of CMMT of the order of 3–5 °C compared to temperatures before and after the MCO, are the most significant parameter indicating MCO palaeoclimate alteration in the coastal lowlands in central and eastern Germany. MAP values for the three fossil sites are consistently above 1,000 mm, but not as high (2,000 mm) as has been assumed from qualitative interpretations of the Wiesa flora. In contrast to CA- and BA-derived estimates, IA/ODA palaeoclimate values indicate Cwa/b climate types for Wiesa, instead of the Cfa in the Köppen-Geiger system. But precipitation values from BA are close to the transition from Cf to Cw climate. Seasonality in precipitation as is revealed by palaeobotanical approaches (CLAMP, CA, IA/ODA) has not yet been confirmed by non-botanical proxy data, and could be reinforced through incorporation of NLRs from monsoon areas of SE Asia into the calibration datasets. The precipitation parameters consistently indicate wetter summers and drier, but not dry winters.

Acknowledgements

We thank our working group members for any technical support for our research, in particular Carola Kunzmann for cuticle preparations. Karolin Moraweck (Radebeul, Germany), former scientist in LK's group, is cordially acknowledged for conducting CA analysis for the Wiesa assemblage in 2017. Many thanks to Vasilis Teodoridis (Prague, Czech Republic) for supporting the IPR vegetation analysis. Our sincere thanks go to Gerda Standke (Freiberg) and Jochen Rascher (Dresden) for providing the most recent information on the lithostratigraphy of the Wiesa section in the kaoline quarry. LK had many fruitful and stimulating discussions with the late Dieter Hans Mai (Berlin, Germany) on floristic evolution in the Paleogene and Neogene of central Europe. JH acknowledges grants from the National

Natural Science Foundation of China (No. 31800183), the Yunnan Basic Research Projects (No. 2019FB026), and the Chinese Academy of Science "Light of West China" Program. LK is grateful for a visiting grant for collaborative field work in 2016 and 2017 in XTBG. This publication is a contribution to the NECLIME network. Two reviewers and Johanna Kovar-Eder as guest editor of the volume are kindly acknowledged for the valuable recommendations to improve the first version of the manuscript.

References

Andreánsky, G. (1959): Die Flora der sarmatischen Stufe in Ungarn. – Akademiai Kiadó, Budapest, 360 pp.

APG IV (2016): An update of the Angiosperm Phylogeny Group classification for the orders and families of flowering plants: APG IV. – Botanical Journal of the Linnean Society, 181: 1–20. [online access: Angiosperm Phylogeny Website. Version 14, http://www.mobot.org/MOBOT/research/APweb/.] https://doi.org/10.1111/boj.12385

Belda, M., Holtanová, E., Halenka, T., Kalvová, J. (2014): Climate classification revisited: from Köppen to Trewartha. – Climate Research, 59: 1–13. https://doi.org/10.3354/cr01204

Böhme, M., Bruch, A. A., Selmeier, A. (2007): The reconstruction of Early and Middle Miocene climate and vegetation in Southern Germany as determined from the fossil wood flora. – Palaeogeography, Palaeoclimatology, Palaeoecology, 253: 91–114. https://doi.org/10.1016/j.palaeo.2007.03.035

Bondarenko, O. V., Blokhina, N. I., Mosbrugger, V., Utescher, T. (2019): Paleogene climate dynamics in the Primorye Region, Far East of Russia, based on a Coexistence Approach analysis of palaeobotanical data. – Palaeobiodiversity and Palaeoenvironments, 100: 5–31. https://doi.org/10.1007/s12549-019-00377-4

Bruch, A. A., Uhl, D., Mosbrugger, V. (2007): Miocene climate in Europe – patterns and evolution: a first synthesis of NECLIME. – Palaeogeography, Palaeoclimatology, Palaeoecology, 253: 1–7. https://doi.org/10.1016/j.palaeo.2007.03.030

Bruch, A. A., Utescher, T., Mosbrugger, V., NECLIME members (2011): Precipitation patterns in the Miocene of Central Europe and the development of continentality. – Palaeogeography, Palaeoclimatology, Palaeoecology, 304: 202–211. https://doi.org/10.1016/j.palaeo.2010.10.002

Christenhusz, M. J. M., Reveal, J. L., Farjon, A., Gardner, M. F., Mill, R. R., Chase, M. W (2011): A new classification and linear sequence of extant gymnosperms. – Phytotaxa, 19: 55–70. https://doi.org/10.11646/phytotaxa.19.1.3

Climate-Data.org (2021): Klimadaten Tenchong von Climate-data.org. – https://de.climate-data.org. [accessed May 2nd, 2021]

Cohen, K. M., Finney, S. C., Gibbard, P. L., Fan, J.-X. (2013; updated): The ICS International Chronostratigraphic Chart. – Episodes, 36: 199– 204. https://doi.org/10.18814/epiiugs/2013/v36i3/002

Doláková, N., Kováčová, M., Utescher, T. (2021): Vegetation and climate changes during the Miocene climatic optimum and Miocene climatic transition in the northwestern part of Central Paratethys. – Geological Journal, 56: 729–743. https://doi.org/10.1002/gj.4056

Donders, T. H., Weijers, J. W. H., Munsterman, D. K., Kloosterboer-van Hoeve, M. L., Buckles, L. K., Pancost, R. D., Schouten, S., Sinninghe Damsté, J. S., Brinkhuis, H. (2009): Strong climate coupling of terrestrial and marine environments in the Miocene of northwest Europe. – Earth and Planetary Science Letters, 281: 215–225. https://doi.org/10.1016/j.epsl.2009.02.034

Editorial Committee of Vegetation Map of China, The Chinese Academy of Sciences (2007): Vegetation Map of the People's Republic of China (1:1,000,000). – Geological Publishing House, Beijing.

Eldrett, J. S., Greenwood, D. R., Harding, I. C., Huber, M. (2009): Increased seasonality through the Eocene to Oligocene transition in northern high latitudes. – Nature, 459: 969–973. https://doi.org/10.1038/nature08069

Engler, A. (1908): Die Vegetationsformen tropischer und subtropischer Länder. – Botanische Jahrbücher für Systematik, Pflanzengeschichte und Pflanzengeographie, 41: 367–372.

Erdei, B., Utescher, T., Hably, L., Tamás, J., Roth-Nebelsick, A., Grein, M. (2012): Early Oligocene continental climate of the Palaeogene Basin (Hungary and Slovenia) and the surrounding area. – Turkish Journal of Earth Sciences, 21: 153–186.

Escher, D., Gerschel, H., Geißler, M., Hartmann, A., Rascher, J., Rascher, M., Richter, L., Wittwer, S., Standke, G., Pfeiffer, N., Blumenstengel, H. (2020): Neukartierung der Lithofazies-/Horizontkarten Tertiär i. M. 1:50.000 für die sächsische Lausitz (LKT50 Lausitz). – Sächsisches Landesamt für Umwelt, Landwirtschaft und Geologie, Dresden, 89 pp.

Fauquette, S., Suc, J.-P., Jiménez-Moreno, G., Micheels, A., Jost, A., Favre, E., Bachiri-Taoufiq, N., Bertini, A., Clet-Pellerin, M., Diniz, F., Farjanel, G., Feddi, N., Zheng, Z. (2007): Latitudinal climatic gradients in the Western European and Mediterranean regions from the Mid-Miocene (c. 15 Ma) to the Mid-Pliocene (c. 3.5 Ma) as quantified from pollen data. – In: Williams, M., Haywood, A. M., Gregory, F. J., Schmidt, D. N. (eds), Deep-Time Perspectives on Climate Change: Marrying the Signal from Computer Models and Biological Proxies. The Micropalaeontological Society, Special Publications; The Geological Society, London, pp. 481–502. https://doi.org/10.1144/TMS002.22

Flower, B. P., Kennett, J. P. (1994): The middle Miocene climatic transition: East Antarctic ice sheet development, deep ocean circulation and global carbon cycling. – Palaeogeography, Palaeoclimatology, Palaeoecology, 108: 537–555. https://doi.org/10.1016/0031-0182(94)90251-8

Gastaldo, R. A., Ferguson, D. K., Walther, H., Rabold, J. M. (1996): Criteria to distinguish parautochthonous leaves in Tertiary alluvial channel-fills. – Review of Palaeobotany and Palynology, 91: 1–21. https://doi.org/10.1016/0034-6667(95)00071-2

Geiger, R. (1954): Klassifikationen der Klimate nach W. Köppen. – In: Landolf-Börnstein: Zahlenwerte und Funktionen aus Physik, Chemie, Astronomie, Geophysik und Technik (alte Serie), Vol. 3. Springer, Berlin, pp. 603−607.

Greenwood, D. R., Wing, S. L. (1995): Eocene continental climates and latitudinal temperature gradients. – Geology, 23: 1044–1048. https://doi.org/10.1130/0091-7613(1995)023<1044:ECCALT>2.3.CO;2

Grein, M., Oehm, C., Konrad, W., Utescher, T., Kunzmann, L., Roth-Nebelsick, A. (2013): Atmospheric CO_2 from the late Oligocene to early Miocene based on photosynthesis data and fossil leaf characteristics. – Palaeogeography, Palaeoclimatology, Palaeoecology, 374: 41–51. https://doi.org/10.1016/j.palaeo.2012.12.025

Grimm, G. W., Denk, T. (2012): Reliability and resolution of the coexistence approach – Revalidation using modern-day data. – Review of Palaeobotany and Palynology, 172: 33–47. https://doi.org/10.1016/j.revpalbo.2012.01.006

Holbourn, A. E., Kuhnt, W., Kochhann, K. G. D., Andersen, N., Meier, K. J. S. (2015): Global perturbation of the carbon cycle at the onset of the Miocene climatic optimum. – Geology, 43(2): 123–126. https://doi.org/10.1130/G36317.1

Holý, F., Kvaček, Z., Teodoridis, V. (2012): A review of the early Miocene mastixioid flora of the Kristina Mine at Hrádek nad Nisou in North Bohemia (Czech Republic). – Acta Musei Nationalis Pragae, Series B – Historia Naturalis, 68(3-4): 53–118.

Hutchinson, D. K., Coxall, H. K., Lunt, D. J., Steinthorsdottir, M., de Boer, A. M., Baatsen, M., von der Heydt, A., Huber, M., Kennedy-Asser, A. T., Kunzmann, L., Ladant, J.-B., Lear, C. H., Moraweck, K., Pearson, P. N., Piga, E., Pound, M. J., Salzmann, U., Scher, H. D., Sijp, W. P., Śliwińska, K. K., Wilson, P. A., Zhang, Z. (2021): The Eocene–Oligocene transition: a review of marine and terrestrial proxy data, models and model-data comparisons. – Climate of the Past, 17: 269–315. https://doi.org/10.5194/cp-17-269-2021

Inglis, G. N., Bragg, F., Burls, N. J., Cramwinckel, M. J., Evans, D., Foster, G. L., Huber, M., Lunt, D. J., Siler, N., Steinig, S., Tierney, J. E., Wilkinson, R., Anagnostou, E., de Boer, A. M., Dunkley Jones, T., Edgar, K. M., Hollis, C. J., Hutchinson, D. K., Pancost, R. D. (2020): Global mean surface temperature and climate sensitivity of the early Eocene Climatic Optimum (EECO), Paleocene-Eocene Thermal Maximum (PETM), and latest Paleocene. – Climate of the Past, 16: 1953–1968. https://doi.org/10.5194/cp-16-1953-2020

Ivanov, D., Utescher, T., Mosbrugger, V., Syabryaj, S., Djordjević-Milutinović, D., Molchanoff, S. (2011): Miocene vegetation and climate dynamics in Eastern and Central Paratethys (Southeastern Europe). – Palaeogeography, Palaeoclimatology, Palaeoecology, 304: 262–275. https://doi.org/10.1016/j.palaeo.2010.07.006

Kershaw, A. P. (1997): A bioclimatic analysis of early to middle Miocene brown coal floras, Latrobe Valley, south-eastern Australia. – Australian Journal of Botany, 45: 373–387. https://doi.org/10.1071/BT96033

Kirchheimer, F. (1938): Beiträge zur näheren Kenntnis der Mastixioideen-Flora des deutschen Mittel- bis Oberligozäns. – Beihefte Botanisches Centralblatt, Abteilung B, 58: 303–375.

Konrad, W., Roth-Nebelsick, A., Grein, M. (2008): Modelling stomatal density response to atmospheric CO_2. – Journal of Theoretical Biology, 253(4): 638–658. https://doi.org/10.1016/j.jtbi.2008.03.032

Köppen, W. (1900): Versuch einer Klassifikation der Klimate, vorzugsweise nach ihren Beziehungen zur Pflanzenwelt. – Geographische Zeitschrift, 6: 593–611, 657–679.

Köppen, W. (1936): Das geographische System der Klimate. – In: Köppen, W., Geiger, G. (eds.), Handbuch der Klimatologie. Gebrüder Borntraeger, Berlin, pp. 1–44.

Kottek, M., Grieser, J., Beck, C., Rudolf, B., Rubel, F. (2006): World Map of the Köppen-Geiger climate classification updated. – Meteorologische Zeitschrift, 15: 259–263. https://doi.org/10.1127/0941-2948/2006/0130

Kovar-Eder, J., Jechorek, H., Kvaček, Z., Parashiv, V. (2008): The Integrated Plant Record: an essential tool for reconstructing Neogene zonal vegetation in Europe. – Palaios, 23: 97–111. https://doi.org/10.2110/palo.2006.p06-039r

Kovar-Eder, J., Kvaček, Z. (2003): Towards vegetation mapping based on the fossil plant record. – Acta Universitatis Carolinae, Geologica, 46(4): 7–13.

Kovar-Eder, J., Kvaček, Z. (2007): The integrated plant record (IPR) to reconstruct Neogene vegetation: The IPR-vegetation analysis. – Acta Palaeobotanica, 47(2): 391–418.

Kovar-Eder, J., Mazouch, P., Teodoridis, V., Roth-Nebelsick, A., Traiser, C., Wypich, J. (2021): Modern vegetation proxies reflect Palaeogene and Neogene vegetation evolution and climate change in Europe, Turkey, and Armenia. – Palaeontologia Electronica, 24(2): a18. https://doi.org/10.26879/1131

Kovar-Eder, J., Teodoridis, V. (2018): The middle Miocene Central European plant record revisited; widespread subhumid sclerophyllous forests indicated. – Fossil Imprint, 74(1-2): 115–134. https://doi.org/10.2478/if-2018-0009

Krutzsch, W. (2000): Stratigraphische Tabelle Oberoligozän und Neogen (marin – kontinental). – Berliner geowissenschaftliche Abhandlungen, Reihe E, 34: 153–165.

Krutzsch, W. (2011): Stratigrafie und Klima des Paläogens im Mitteldeutschen Ästuar im Vergleich zur marinen nördlichen Umrahmung. – Zeitschrift der deutschen Gesellschaft für Geowissenschaften, 162: 19–46. https://doi.org/10.1127/1860-1804/2011/0162-0019

Kryshtofovich, A. N. (1929): Evolution of the Tertiary Flora in Asia. – New Phytologist, 28(4): 303–312. https://doi.org/10.1111/j.1469-8137.1929.tb06761.x

Kunzmann, L. (2014): On the fossil history of Pseudotsuga Carr. (Pinaceae) in Europe. – Palaeobiodiversity and Palaeoenvironments, 94: 393–409. https://doi.org/10.1007/s12549-014-0156-x

Kunzmann, L., Kvaček, Z., Teodoridis, V., Müller, C., Moraweck, K. (2016): Vegetation dynamics of riparian forest in central Europe during the late Eocene. – Palaeontographica, Abteilung B, 295: 69–89. https://doi.org/10.1127/palb/295/2016/69

Kunzmann, L., Mai, D. H. (2005): Die Koniferen der Mastixioideen-Flora von Wiesa bei Kamenz (Sachsen, Miozän) unter besonderer Berücksichtigung der Nadelblätter. – Palaeontographica, Abteilung B, 272(1-6): 67–135. https://doi.org/10.1127/palb/272/2005/67

Kunzmann, L., Müller, C., Moraweck, K., Bräutigam, D., Wappler, T., Nel, A. (2017): First record of insects in lignite-bearing formations (upper Eocene) of the central German Leipzig Embayment. – Paläontologische Zeitschrift 91: 315–326. https://doi.org/10.1007/s12542-017-0367-3

Kürschner, W. M., Kvaček, Z., Dilcher, D. L. (2008): The impact of Miocene atmospheric carbon dioxide fluctuations on climate and the evolution of terrestrial ecosystems. – Proceedings of the National Academy of Sciences, 105: 449–453. https://doi.org/10.1073/pnas.0708588105

Kvaček, Z. (2010): Forest flora and vegetation of the European early Paleogene – a review. – Bulletin of Geosciences, 85(1): 63–76. https://doi.org/10.3140/bull.geosci.1146

Kvaček, Z., Kovác, M., Kovar-Eder, J., Doláková, N., Jechorek, H., Parashiv, V., Kováčová, M., Sliva, L. (2006): Miocene evolution of landscape and vegetation in the Central Paratethys. – Geologica Carpathica, 57: 295–310.

Kvaček, Z., Manchester, S. R., Zetter, R., Pingen, M. (2002): Fruits and seeds of *Craigia bronnii* (Malvaceae – Tilioideae) and associated flower buds from the late Miocene Inden Formation, Lower Rhine basin, Germany. – Review of Palaeobotany and Palynology, 119: 311–324. https://doi.org/10.1016/S0034-6667(01)00135-X

Kvaček, Z., Teodoridis, V., Zajícová, J. (2015): Revision of the early Oligocene flora of Hrazený hill (formerly Pirskenberg) in Knížecí near Šluknov, North Bohemia. – Acta Musei Nationalis Pragae, Series B – Historia Naturalis, 71(1-2): 55–102. https://doi.org/10.14446/AMNP.2015.55

Kvaček, Z., Walther, H. (2001): The Oligocene in Central Europe and the development of forest vegetation in space and time based on megafossils. – Palaeontographica, Abteilung B, 259(1-6), 125–148.

Larsson, L. M., Dybkjær, K., Rasmussen, E. S., Piasecki, S., Utescher, T., Vajda, V. (2011): Miocene climate evolution of northern Europe: A palynological investigation from Denmark. – Palaeogeography, Palaeoclimatology, Palaeoecology, 309: 161–175. https://doi.org/10.1016/j.palaeo.2011.05.003

Li, S.-F., Mao, L.-M., Spicer, R. A., Lebreton-Anberrée, J., Su, T., Sun, M., Zhou, Z.-K. (2015): Late Miocene vegetation dynamics under monsoonal climate in southwestern China. – Palaeogeography, Palaeoclimatology, Palaeoecology, 425: 14–40. https://doi.org/10.1016/j.palaeo.2015.02.030

Li, S.-F., Xing, Y., Valdes, P. J., Huang, Y.-J., Su, T., Farnsworth, A., Lunt, D. J., Tang, H., Kennedy, A. T., Zhou, Z.-K. (2018): Oligocene climate signals and forcings in Eurasia revealed by plant macrofossil and modelling results. – Gondwana Research, 61: 115–127. https://doi.org/10.1016/j.gr.2018.04.015

Mai, D. H. (1964): Die Mastixioideen-Floren im Tertiär der Oberlausitz. – Paläontologische Abhandlungen, Reihe B, II(1): 1–192.

Mai, D. H. (1967): Die Florenzonen, der Florenwechsel und die Vorstellungen über den Klimaablauf im Jungtertiär der DDR. – Abhandlungen des Zentralen Geolologischen Instituts Berlin, 10: 55–81.

Mai, D. H. (1993): On the extinct Mastixiaceae (Cornales) in Europe. – Geophytology, 23: 53–63.

Mai, D. H. (1995): Tertiäre Vegetationsgeschichte Europas – Methoden und Ergebnisse. – G. Fischer, Jena, Stuttgart, New York, 691 pp.

Mai, D. H. (1998): Contributions to the flora of the middle Oligocene Calau Beds in Brandenburg, Germany. – Review of Palaeobotany and Palynology, 101: 43–70. https://doi.org/10.1016/S0034-6667(97)00069-9

Mai, D. H. (1999a): Die untermiozänen Floren aus der Spremberger Folge und dem 2. Flözhorizont in der Lausitz. Teil I: Farnpflanzen, Koniferen und Monokotyledonen. – Palaeontographica, Abteilung B, 250: 1–76.

Mai, D. H. (1999b): Die untermiozänen Floren aus der Spremberger Folge und dem 2. Flözhorizont in der Lausitz. Teil II: Polycarpicae und Apetalae. – Palaeontographica, Abteilung B, 251(1-3): 1–70.

Mai, D. H. (2000a): Die untermiozänen Floren aus der Spremberger Folge und dem 2. Flözhorizont der Lausitz. Teil III. Dialypetalae und Sympetalae. – Palaeontographica, Abteilung B, 253(1-3): 1–106.

Mai, D. H. (2000b): Die untermiozänen Floren aus der Spremberger Folge und dem 2. Flözhorizont in der Lausitz. Teil IV: Fundstellen und Paläobiologie. – Palaeontographica, Abteilung B, 254: 65–176. https://doi.org/10.1127/palb/254/2000/65

Mai, D. H. (2001a): Die mittelmiozänen und obermiozänen Floren aus der Meuroer und Raunoer Folge in der Lausitz. Teil II: Dicotyledonen. – Palaeontographica, Abteilung B, 257(1-6): 35–174.

Mai, D. H. (2001b): Die mittelmiozänen und obermiozänen Floren aus der Meuroer und Raunoer Folge in der Lausitz. Teil III: Fundstellen und Paläobiologie. – Palaeontographica, Abteilung B, 258(1-3): 1–85.

Mai, D. H., Martinetto, E. (2006): A reconsideration of the diversity of *Symplocos* in the European Neogene on the basis of fruit morphology. – Review of Palaeobotany and Palynology, 140: 1–26. https://doi.org/10.1016/j.revpalbo.2006.02.001

Mai, D. H., Walther, H. (1991): Die oligozänen und untermiozänen Floren NW-Sachsens und des Bitterfelder Raumes. – Abhandlungen des Staatlichen Museums für Mineralogie und Geologie Dresden, 38: 1–230.

Manchester, S. R., Fritsch, P. W. (2014): European fossil fruits of *Sphenotheca* related to extant Asian species of *Symplocos*. – Journal of Systematics and Evolution, 52(1): 68–74. https://doi.org/10.1111/jse.12060

Martinetto, E. (2001): The role of central Italy as a centre of refuge for thermophilous plants in the late Cenozoic. – Acta Palaeobotanica, 41(2): 299–319.

Methner, K., Campani, M., Fiebig, J., Löffler, N., Kempf, O., Mulch, A. (2020): Middle Miocene long-term continental temperature change in and out of

pace with marine climate records. – Scientific Reports, 10: 7989 (10 pp).
https://doi.org/10.1038/s41598-020-64743-5

Meyer, C., Weigelt, P., Kreft, H. (2016): Multidimensional Biases, Gaps and Uncertainties in Global Plant Occurrence Information. – Ecology Letters, 19(8): 992–1006.
https://doi.org/10.1111/ele.12624

Moraweck, K., Grein, M., Konrad, W., Kvaček, J., Kovar-Eder, J., Neinhuis, C., Traiser, C., Kunzmann, L. (2019): Leaf traits of long-ranging Paleogene species and their relationship with depositional facies, climate and atmospheric CO_2 level. – Palaeontographica, Abteilung B, 298: 93–172.
https://doi.org/10.1127/palb/2019/0062

Mosbrugger, V. (1999): The nearest living relative method. – In: Jones, T. P., Rowe, N. P. (eds), Fossil Plants and Spores: Modern Techniques. Geological Society, London, pp. 261– 265.

Mosbrugger, V., Utescher, T. (1997): The coexistence approach – a method for quantitative reconstructions of Tertiary terrestrial palaeoclimate data using plant fossils. – Palaeogeography, Palaeoclimatology, Palaeoecology, 134: 61–86.
https://doi.org/10.1016/S0031-0182(96)00154-X

Mosbrugger, V., Utescher, T., Dilcher, D. L. (2005): Cenozoic continental climatic evolution of Central Europe. – Proceedings of the National Academy of Sciences, 102(42): 14964–14969.
https://doi.org/10.1073/pnas.0505267102

Oh, I.-C., Denk, T., Friis, E. M. (2003): Evolution of *Illicium* (Illicaceae): Mapping morphological characters on the molecular tree. – Plant Systematics and Evolution, 240: 175–209.
https://doi.org/10.1007/s00606-003-0022-1

PALAEOFLORA (2018): Data Base for Palaeoclimate Reconstructions Using the Coexistence Approach. – http://www.palaeoflora.de. [accessed on February 1st, 2021]

Palazzesi, L., Barreda, V. D., Cuitiño, J. I., Guler, M. V., Tellería, M. C., Ventura Santos, R. (2014): Fossil pollen records indicate that Patagonian desertification was not solely a consequence of Andean uplift. – Nature Communications, 5: 1–8.
https://doi.org/10.1038/ncomms4558

Peel, M. C., Finlayson, B. L., McMahan, T. A. (2007): Updated World Map of Köppen-Geiger Climate Classification. – Hydrology and Earth System Sciences, 11: 1633–1644.
https://doi.org/10.5194/hess-11-1633-2007

Popova, S., Utescher, T., Gromyko, D. V., Bruch, A. A., Henrot, A.-J., Mosbrugger, V. (2017): Cenozoic vegetation gradients in the mid- and higher latitudes of Central Eurasia and climatic implications. – Palaeogeography, Palaeoclimatology, Palaeoecology, 467: 69–82.
https://doi.org/10.1016/j.palaeo.2016.09.016

Pound, M. J., Haywood, A. M., Salzmann, U., Riding, J. B. (2012): Global vegetation dynamics and latitudinal temperature gradients during the Mid to Late Miocene (15.97–5.33 Ma). – Earth-Science Review, 112: 1–22.
https://doi.org/10.1016/j.earscirev.2012.02.005

Pound, M. J., Salzmann, U. (2017): Heterogeneity in global vegetation and terrestrial climate change during the late Eocene to early Oligocene transition. – Scientific Reports, 7, 43386.
https://doi.org/10.1038/srep43386

Prebble, J. G., Reichgelt, T., Mildenhall, D. C., Greenwood, D. R., Raine, J. I., Kennedy, E. M., Seebeck, H. C. (2017): Terrestrial climate evolution in the Southwest Pacific over the past 30 million years. Earth Planet. – Scientific Letters, 459: 136–144.
https://doi.org/10.1016/j.epsl.2016.11.006

Reichgelt, T., Kennedy, E. M., Mildenhall, D. C., Conran, J. G., Greenwood, D. R., Lee, D. E. (2013): Quantitative palaeoclimate estimates for Early Miocene southern New Zealand: Evidence from Foulden Maar. – Palaeogeography, Palaeoclimatology, Palaeoecology, 378: 36–44.
https://doi.org/10.1016/j.palaeo.2013.03.019

Rothmaler, W. (1938): Systematik und Geographie der Subsektion *Cotlycanthum* der Gattung *Alchemilla* L. – Repertorium Specierum Novarum Regni Vegetabilis, Beihefte 100: 59–93.

Spicer, R. A., Valdes, P. J., Spicer, T. E. V., Craggs, H. J., Srivastava, G., Mehrotra, R. C., Yang, J. (2009): New developments in CLAMP: calibration using global gridded meteorological data. – Palaeogeography, Palaeoclimatology, Palaeoecology, 283(1-2): 91–98.
https://doi.org/10.1016/j.palaeo.2009.09.009

Standke, G. (2008): Tertiär. – In: Pälchen, W., Walther, H. (eds), Geologie von Sachsen, Geologischer Bau und Entwicklungsgeschichte. E. Schweizerbart'sche Verlagsbuchhandlung, Stuttgart, pp. 358–419.

Standke, G., Escher, D., Fischer, J., Rascher, J. (2010): Das Tertiär Nordwestsachsens. Ein geologischer Überblick. – Landesamt für Umwelt, Landwirtschaft und Geologie, Radebeul, Dresden, Freiberg, 160 pp.

Steinthorsdottir, M., Jardine, P. E., Rember, W. C. (2021): Near future pCO_2 during the hot Miocene climatic optimum. – Paleoceanography and Paleoclimatology, 36: e2020PA003900 (15 pp.).
https://doi.org/10.1029/2020PA003900

Striegler, U. (2017): Die obermiozäne Flora des Blättertones von Wischgrund und anderer gleichaltriger Fundstellen der Klettwitzer Hopchfläche (Niederlausitz, Land Brandeburg, Deutschland). – Peckiana, 12: 1–151.

Su, T., Xing, Y.-W., Liu, Y.-S., Jacques, F. M. B., Chen, W.-Y., Huang, Y.-J., Zhou, Z.-K. (2010): Leaf Margin Analysis: A new equation from humid to mesic forests in China. – Palaios, 25: 234–238.
https://doi.org/10.2110/palo.2009.p09-129r

Teodoridis, V., Kovar-Eder, J., Marek, P., Kvaček, Z., Mazouch, P. (2011): The Integrated Plant Record Vegetation Analysis: Internet Platform and Online Application. – Acta Musei nationalis Pragae, Series B – Historia Naturalis, 67(3-4): 159–164.

Teodoridis, V. (2004): Floras and vegetation of Tertiary fluvial sediments of Central and Northern Bohemia and their equivalents in deposits of the Most Basin (Czech Republic). – Acta Musei nationalis Pragae, Series B – Historia Naturalis, 60(3-4): 113–142.

Teodoridis, V., Kovar-Eder, J., Marek, P., Mazouch, P., Kvaček, Z. (2011–2021): IPR database. http://www.ipr-database.eu/. – Faculty of Education, Charles University, Prague.

Teodoridis, V., Kvaček, Z. (2015): Palaeoenvironmental evaluation of Cainozoic plant assemblages from the Bohemian Massif (Czech Republic) and adjacent Germany. – Bulletin of Geosciences, 90(3): 695–720. https://doi.org/10.3140/bull.geosci.1553

Teodoridis, V., Marek, P., Mazouch, P., Kovar-Eder, J. (2020–2021): Online application of Drudge 1 and 2. http://www.iprdatabase.eu/drudges/new/. – Faculty of Education, Charles University, Prague. [accessed on November 23, 2021]

Teodoridis, V., Mazouch, P., Kovar-Eder, J. (2020): The Integrated Plant Record (IPR) analysis: Methodological advances and new insights into the evolution of European Palaeogene/Neogene vegetation. – Palaeontologia Electronica, 23(1): a16 (19 pp.). https://doi.org/10.26879/1055

Teodoridis, V., Mazouch, P., Kovar-Eder, J. (2021): On-line application of Drudge 1 and 2 – simple and quick determination of the modern vegetation most closely resembling fossil plant assemblages. – Neues Jahrbuch für Geologie und Paläontologie, Abhandlungen, 299(1): 71–75. https://doi.org/10.1127/njgpa/2021/0955

Thompson, R. S., Anderson, K. H., Pelltier, R. T., Strickland, L. E., Bartlein, P. J., Shafer, S. L. (2012): Quantitative estimation of climatic parameters from vegetation data in North America by the mutual climatic range technique. – Journal of Quaternary Science, 51: 18–39. https://doi.org/10.1016/j.quascirev.2012.07.003

Trewartha, G. T. (1968): An introduction to climate. – McGraw-Hill, New York, 408 pp.

Trewartha, G. T., Horn, L. H. (1980): Introduction to climate, 5th ed. – McGraw-Hill, New York, 416 pp.

Uhl, D. (2006): Fossil plants as palaeoenvironmental proxies – some remarks on selected approaches. – Acta Palaeobotanica, 46(2): 87–100.

Uhl, D., Mosbrugger, V., Bruch, A., Utescher, T. (2003): Reconstructing palaeotemperatures using leaf floras – case studies for a comparison of leaf margin analysis and the coexistence approach. – Review of Palaeobotany and Palynology, 126: 49–64. https://doi.org/10.1016/S0034-6667(03)00058-7

Utescher, T., Ashraf, A. R., Dreist, A., Dybkjær, K., Mosbrugger, V., Pross, J., Wilde, V. (2012): Variability of Neogene continental climates in Northwest Europe – a detailed study based on microfloras. – Turkish Journal of Earth Sciences, 21: 289–314.

Utescher, T., Ashraf, A. R., Kern, A. K., Mosbrugger, V. (2021): Diversity patterns in microfloras recovered from Miocene brown coals of the lower Rhine Basin reveal distinct coupling of the structure of the peat forming vegetation and continental climate variability. – Geological Journal, 56: 768–785. https://doi.org/10.1002/gj.3801

Utescher, T., Bruch, A. A., Micheels, A., Mosbrugger, V., Popova, S. (2011): Cenozoic climate gradients in Eurasia – a palaeo-perspective on future climate change? – Palaeogeography, Palaeoclimatology, Palaeoecology, 304: 351–358. https://doi.org/10.1016/j.palaeo.2010.09.031

Utescher, T., Bruch, A., Erdei, B., François, L., Ivanov, D., Jacques, F. M. B., Kern, A. K., Liu, Y., Mosbrugger, V., Spicer, R. A. (2014): The Coexistence Approach – theoretical background and practical considerations of using plant fossils for climate quantification. – Palaeogeography Palaeoclimatology Palaeoecology, 410: 58–73. https://doi.org/10.1016/j.palaeo.2014.05.031

Utescher, T., Dreist, A., Henrot, A.-J., Hickler, T., Liu (C.) Y.-S., Mosbrugger, V., Portmann, F. T., Salzmann, U. (2017): Continental climate gradients in North America and Western Eurasia before and after the closure of the Central American Seaway. – Earth and Planetary Science Letters, 472: 120–130. https://doi.org/10.1016/j.epsl.2017.05.019

Utescher, T., Gebka, M., Mosbrugger, V., Schilling, H.-D., Ashraf, A. (1997): Regional palaeontological-meteorological palaeoclimate reconstruction of the Neogene Lower Rhine Embayment. – Mededelingen Nederlands Instituut voor Toegepaste Geowetenschappen, 58: 263–271.

Utescher, T., Mosbrugger, V., Ivanov, D., Dilcher, D. L. (2009): Present-day climatic equivalents of European Cenozoic climates. – Earth and Planetary Science Letters, 284: 544–552. https://doi.org/10.1016/j.epsl.2009.05.021

Vomela, S. (2016): Die Mikroflora der untermiozänen Fundstelle Wiesa bei Kamenz, Deutschland; MSc thesis. – MS, University of Vienna, Vienna, 167 pp. (in German) (online resource: http://othes.univie.ac.at/41942/1/2016-04-25_0349120.pdf)

Walther, H. (1984): Paläobotanische Sammeltätigkeit im Tertiär der Oberlausitz (1866–1983). – Abhandlungen und Berichte des Naturkundemuseums Görlitz, 58(2): 23–32.

Wang, L., Kunzmann, L., Su, T., Xing, Y.-W., Zhang, S.-T., Wang, Y.-Q., Zhou, Z.-K. (2019): The disappearance of *Metasequoia* (Cupressaceae) after the middle Miocene in Yunnan, Southwest China: Evidences for evolutionary stasis and intensification of the Asian monsoon. – Review of Palaeobotany and Palynology, 264: 64–74. https://doi.org/10.1016/j.revpalbo.2018.12.007

Westerhold, T., Marwan, N., Drury, A. J., Liebrand, D., Agnini, C., Anagnostou, E., Barnet, J., Bohaty, S., De Vleeschouwer, D., Fabio, F., Frederichs, T., Hodell, D., Holbourn, A., Kroon, D., Lauretano, V., Littler, K., Lourens, L., Lyle, M., Pälike, H., Zachos, J. C. (2020): An astronomically dated record of Earth's climate and its predictability over the last 66 million years. – Science, 369: 1383 – 1387. https://doi.org/10.1126/science.aba6853

Wing, S. L., Greenwood, D. R. (1993): Fossils and fossil climate: the case for equable continental interiors in the Eocene. – Royal Society of London Philosophical Transactions, Series B, 341: 243–252. https://doi.org/10.1098/rstb.1993.0109

Wolfe, J. A. (1979): Temperature parameters of humid to mesic forests of eastern Asia and their relation to forests of other areas of the Northern Hemisphere and Australasia. – Geological Professional Paper, 1106: 1– 37. https://doi.org/10.3133/pp1106

Wolfe, J. A. (1993): A method of obtaining climatic parameters from leaf assemblages. – US Government Printing Office, 2040-2041: 1–70.

Yang, J., Spicer, R. A., Spicer, T. E. V., Li, C.-S. (2011): 'CLAMP Online': a new web-based palaeoclimate tool and its application to the terrestrial Paleogene and Neogene of North America. – Palaeobiodiversity and Palaeoenvironments, 91(3): 163–183. https://doi.org/10.1007/s12549-011-0056-2

Yang, J., Wang, Y.-F., Spicer, R. A., Mosbrugger, V., Li, C.-S., Sun, Q.-G. (2007): Climatic reconstruction at the Miocene Shanwang basin, China, using leaf margin analysis, CLAMP, coexistence approach, and overlapping distribution analysis. – American Journal of Botany, 94(4): 599–608. https://doi.org/10.3732/ajb.94.4.599

You, Y., Huber, M., Müller, D. R., Poulsen, C. J., Ribbe, J. (2009): Simulation of the Middle Miocene climate optimum. – Geophysical Research Letters, 36 (4): L04702 (5 pp). https://doi.org/10.1029/2008GL036571

Zachos, J. C., Pagani, M., Sloan, L., Thomas, E., Billups, K. (2001): Trends, Rhythms, and Aberrations in Global Climate 65 Ma to Present. – Science, 292(5517): 686–693. https://doi.org/10.1126/science.1059412

Zachos, J. C., Dickens, G. R., Zeebe, R. E. (2008): An early Cenozoic perspective on greenhouse warming and carbon-cycle dynamics. – Nature, 451(17): 279–283. https://doi.org/10.1038/nature06588

Zhang, J.-W., D'Rozario, A., Adams, J. M., Li, Y., Liang, X.-Q., Jacques, F. M., Su, T., Zhou, Z.-K. (2015): *Sequoia maguanensis*, a new Miocene relative of the coast redwood, *Sequoia sempervirens*, from China: Implications for palaeogeography and palaeoclimate. – American Journal of Botany, 102(1): 103–118. https://doi.org/10.3732/ajb.1400347

Appendix I

Comparison of late Early Miocene flora of Wiesa with stratigraphically older and younger floras in central and eastern Germany. [1] system of gymnosperm families according to Christenhusz et al. 2011; system of angiosperm families according to APG IV 2016; [2] based on Mai and Walther 1991 with updates by Kvaček and Walther 2001, Moraweck et al. 2019; [3] based on Mai 2000b with updates by Kunzmann and Mai 2005, Mai and Martinetto 2006, Kunzmann 2014; [4] based on Striegler 2017; [5] not *Illicium* after Oh et al. 2003, currently undeterminable due to insufficient preservation.

	late Oligocene	late Early Miocene	Late Miocene
Class or order / Family[1] / Fossil-species	Borna-Ost/Bockwitz TC[2]	Wiesa[3]	Wischgrund[4]
Pteridophyta			
Pteridaceae			
"*Pteris*" *satyrorum*		**X**	
Osmundaceae			
Osmunda parschlugiana			**X**
Salviniaceae			
Salvinia cerebrata / *S. reussii*	**X**		
Selaginellaceae			
Selaginella germanica		**X**	
Selaginella saxonica	**X**		
Coniferophyta			
Pinaceae			
Abies resinosa		**X**	
Cathaya bergeri / *C. roseltii*		**X**	
Keteleeria hoehnei		**X**	
Nothotsuga protogaea	**X**	**X**	
Picea beckii	**X**		
Piceoxylon thierbachense	**X**		
Pinus echinostrobus	**X**		
Pinus grossana		**X**	
Pinus hampeana		**X**	**X**
Pinus sp. cf. *P. hepios*	**X**		**X**
Pinus sp. cf. *P. palaeostrobus*	**X**	**X**	
Pinus pseudostrobus	**X**	**X**	**X**
Pinus sp. cf. *P. rigios*			**X**
Pinus sp. (folia)			**X**
Pityophyllum wiesaense		**X**	
Pseudolarix schmidtgenii	**X**	**X**	
Pseudotsuga jechorekiae		**X**	
Tsuga schmidtiana / *T. moenana*	**X**	**X**	
Tsuga schneideriana / *T.* sp.	**X**	**X**	
Cupressaceae			
Cunninghamia miocenica	**X**		
Glyptostrobus brevisiliquata / *G. europaeus*	**X**		
Quasisequoia couttsiae	**X**	**X**	
Sequoia abietina	**X**	**X**	**X**
Taxodium dubium	**X**		**X**
Tetraclinis salicornioides / *T. brongniardtii*	**X**	**X**	**X**
Taxaceae			
Cephalotaxus multiserialis	**X**		
Cephalotaxus ex gr. *harringtonia*			**X**
Taxus engelhardtii		**X**	
Torreya bilinica		**X**	
Ginkgophyta			
Ginkgoaceae			
Ginkgo adiantoides		**X**	
"Basal Dicots"			
Cabombaceae			

	late Oligocene	late Early Miocene	Late Miocene
Class or order / Family[1] / Fossil-species	Borna-Ost/Bockwitz TC[2]	Wiesa[3]	Wischgrund[4]
Nymphaeaceae			
Eoeuryale germanica			**X**
Nuphar sp. cf. *N. canaliculatum*		**X**	
Schisandraceae			
"*Illicum*" *germanicum*[5]		**X**	
Illicium monospermum	**X**		
Magnoliaceae			
Liriodendron fragilis	**X**	**X**	
Liriodendron geminata		**X**	
Magnolia burseracea	**X**	**X**	
Magnolia kristinae			**X**
Magnolia maii	**X**		
Magnolia ludwigii		**X**	**X**
Magnolia parthensis	**X**		
Magnolia sp. (folia)		**X**	
Manglietia germanica	**X**		
Calycanthaceae			
Calycanthus lusaticus			**X**
Lauraceae			
Cinnamomum costatum / *Daphnogene bilinica*		**X**	
Daphnogene cinnamomofolia	**X**		
Laurinoxylon bergeri		**X**	
Laurinoxylon endiandroid		**X**	
Laurinoxylon hasenbergense		**X**	
Laurinoxylon litseoides		**X**	
Laurinoxylon microtracheale		**X**	
Laurocarpum sp.	**X**		
Laurophyllum acutimontanum	**X**		
Laurophyllum medimontanum	**X**		
Ocotea rhenana / *Laurophyllum pseudoprinceps*	**X**	**X**	
Sassafras ferretianum			**X**
Saururaceae			
Saururus bilobatus	**X**		
Monocots			
Araceae			
Epipremnites ornatus	**X**		
Epipremnites reniculus		**X**	**(X)**
Urospathites dalgasii		**X**	
Hydrocharitaceae			
Stratiotes amarus	**X**		
Stratiotes kaltennordheimensis			**(X)**
Stratiotes schaarschmidtii	**X**		
Vallisneria ovalis	**X**		
Smilacaceae			
aff. *Smilax*	**X**		**X**
Alismataceae			
Alisma crassicarpum		**X**	
cf. *Alisma*			**X**
Caldesia proventita		**X**	
Potamogetonaceae			
Potamogeton wiesaensis		**X**	
Dioscoreaceae			
Dioscorea liblarensis		**X**	
Palmae			
Calamus daemonorops		**X**	

	late Oligocene	late Early Miocene	Late Miocene
Class or order / Family[1] / Fossil-species	Borna-Ost/Bockwitz TC[2]	Wiesa[3]	Wischgrund[4]
Monochoria striatella		**X**	
Typhaceae			
Sparganium camenzianum		**X**	
Sparganium haentzschelii		**X**	
Sparganium intermedium	**X**		
Sparganium nanum		**X**	
Sparganium pussilloides	**X**		
Typha tambovica			**(X)**
Xyridaceae			
Xyris lusatica			**(X)**
Cyperaceae			
Carex limosioides		**X**	
Caricoidea jugata	**X**		
Cladiocarya europaea	**X**		
Cladiocarya trebovensis	**X**		
Dulichium hartzianum	**X**		
Dulichium marginatum		**X**	
Scirpus khachlovii	**X**	**X**	
Cyperaceae div. spp.			**(X)**
Poaceae vel Cyperaceae (folia)			**X**
Zingiberaceae			
"*Musophyllum*" sp.	**X**		
Spirematospermum wetzleri	**X**		
"Eudicots"			
Ceratophyllaceae			
Ceratophyllum lusaticum			**X**
Ceratophyllum miocenicum			**X**
Lardizabalaceae			
Decaisnea bornensis	**X**		
Menispermaceae			
Sinomenium cantalense		**X**	
Berberidaceae			
Berberis sp.			**X**
Platanaceae			
Platanus neptuni	**X**		
Sabiaceae			
Meliosma miessleri	**X**		
Meliosma wetteraviensis		**X**	
Altingiaceae			
Liquidambar europaea	**X**	**X**	**X**
Liquidambar triloba			**X**
Liquidambar sp.			**X**
Hamamelidaceae			
Corylopsis longehilata		**X**	
Distylium fergussonii		**X**	**X**
Distylium heinickei	**X**		
Fortunearia altenburgensis	**X**		
Fortunearia europaea		**X**	
Parrotia pristina / *P. reidiana*			**X**
Cercidiphyllaceae			
Cercidiphyllum crenatum	**X**		**X**
Halogaraceae			
Proserpinaca brevicarpa	**X**		
Vitaceae			
Ampelopsis malvaeformis		**X**	

	late Oligocene	late Early Miocene	Late Miocene
Class or order / Family[1] / Fossil-species	Borna-Ost/Bockwitz TC[2]	Wiesa[3]	Wischgrund[4]
Parthenocissus boveyana	**X**		
Parthenocissus britannica	**X**	**X**	
Tetrastigma chandleri		**X**	
Tetrastigma lobata		**X**	
Vitis globosa		**X**	
Vitis lusatica	**X**	**X**	
Vitis palaeomuscadinia		**X**	
Vitis strictum	**X**		
Vitis teutonica	**X**	**X**	
Rosaceae			
Crataegus aff. *monogyna*			**X**
Prunus leporimontana		**X**	
Prunus pereger		**X**	
Prunus scharfii	**X**		
Rosa lignitum	**X**		
Rubus laticostatus	**X**	**X**	
Rubus microspermus	**X**		
Rubus semirotundatus	**X**		
Rubus tuganensis	**X**		
Sorbus herzogenrathensis		**X**	
aff. *Pyracantha*			**X**
Pyrus microsperma	**X**		
Pyrus wischneideri			**X**
Rhamnaceae			
Frangula solitaria		**X**	
Paliurus tiliifolius / *P. favonii*			**X**
Zizyphus striatus	**X**	**X**	
Cannabaceae			
Gironniera carinata		**X**	
Trema lusatica		**X**	
Ulmaceae			
Ulmus carpinoides	**X**		
Ulmus fischeri	**X**		**X**
Ulmus ruszovensis			**X**
Ulmus pyramidalis			**X**
Ulmus sp.			**X**
Zelkova zelkovifolia			**X**
Moraceae			
Ficus lutetianoides	**X**		
Ficus potentilloides		**X**	
Urticaceae			
Boehmeria lithuanica			**(X)**
Boehmeria raria		**X**	
Fagaceae			
Castanea sativa			**X**
Eotrigonobalanus furcinervis	**X**		
Fagus deucalionis	**X**		
Fagus menzelii / *F. deucalionis* (incl. aff. *F. menzelii*)			**X**
Fagus saxonica	**X**		
Fagus sp. cf. *F. silesiaca* var. *gozdnicensis*			**X**
Fagus sp.			**X**
Quercus gigas			**X**
Quercus gregori			**X**
Quercus kubinyii			**X**
Quercus lonchites	**X**		

	late Oligocene	late Early Miocene	Late Miocene
Class or order / Family[1] **/** Fossil-species	Borna-Ost/Bockwitz TC[2]	Wiesa[3]	Wischgrund[4]
Quercus pseudocastanea			**X**
Quercus rhenana		**X**	**X**
Quercus schoetzii			**X**
Quercus (*Cyclobalanopsis*) *wischgrundensis*			**X**
Quercus sp. 1			**X**
Quercus sp. (folia)		**X**	
Trigonobalanopsis exacantha / *T. rhamnoides*	**X**	**X**	
Fagaceae div. spp.			**X**
Myricaceae			
Comptonia goniocarpa	**X**		
Coptonia longistyla	**X**		
Myrica boveyana (= *M. wiesaensis*)		**X**	
Myrica cerifériformis		**X**	**X**
Myrica sp. cf. *M. crenata*			**X**
Myrica lignitum			**X**
Myrica stoppii		**X**	
Myrica suppanii		**X**	
Juglandaceae			
Carya bohemica		**X**	
Carya denticulata			**X**
Carya hauffei		**X**	
Carya lusatica		**X**	
Carya serrifolia			**X**
Carya sp.			**X**
Cyclocarya cyclocarpa	**X**	**X**	**X**
Engelhardia orsbergensis		**x**	**(X)**
Pterocarya paradisiaca			**X**
Betulaceae			
Alnus alnoidea			**X**
Alnus sp. cf. *A. ascendens*			**X**
Alnus gaudinii	**X**		
Alnus julianaeformis			**X**
Alnus kefersteinii	**X**		
Alnus latibracteosa	**X**		
Alnus sp. cf. *A. menzelii* / *A. kefersteinii*		**X**	**X**
Alnus rostaniana	**X**		
Alnus sp.			**X**
Betula dryadum	**X**		
Betula sp. cf. *B. plioplatyptera*			**X**
Betula sp.			**X**
Betula sp. cf. *B. subpubescens*			**X**
Carpinus cordataeformis	**X**		
Carpinus grandis	**X**		**X**
Corylus sp. aff. *C. avellana*			**X**
Hypericaceae			
Hypericum miocenicum			**(X)**
Hypericum septestum	**X**		
Passifloraceae			
Passiflora kirchheimeri		**X**	
Salicaceae			
Salix sp. cf. *S. longa*			**X**
Salix varians	**X**		**X**
Populus balsamoides / *P. latior*			**X**
Populus germanica	**X**		
Populus populina			**X**
Populus sp.			**X**

	late Oligocene	late Early Miocene	Late Miocene
Class or order / Family[1] / Fossil-species	Borna-Ost/Bockwitz TC[2]	Wiesa[3]	Wischgrund[4]
Poliothyrsis eurorimosa	**X**		
Euphorbiaceae			
Acalypha fragilis		**X**	
Sapium germanicum		**X**	
Combretaceae			
Quisqualis pentaptera (?*Craigia bronnii*)		**X**	
Onagraceae			
Ludwigia spp.			**(X)**
Lythraceae			
Decodon gibbosus / *Microdiptera menzelii*	**X**	**X**	**X**
Decodon vectensis	**X**		
Hemitrapa heissigii			**X**
Microdiptera lunatic	**X**		
Microdiptera minor	**X**		
Punica antiquorum			**X**
Melastomaceae			
"*Melastomites*" *tertiaries*			
Staphyleaceae			
Turpinia ettingshausenii		**X**	
Sapindaceae			
Acer haselbachense	**X**		
Acer hercynicum	**X**		
Acer integerrimum	**X**		
Acer cf. *integrilobum*			**X**
Acer menzelii			**X**
Acer sp. (fructi et folia)	**X**		**X**
Acer tricuspidatum div. ssp.			**X**
Acer sp. cf. *A. vondobonensis* / *A. polymorphoides*			**X**
Sapindospermum lusaticum	**X**		
Rutaceae			
Phellodendron lusaticum		**X**	
Toddalia maii		**X**	
Malvaceae			
Burretia instructa		**X**	
Byttneriophyllum tiliifolium			**(X)**
Laria sp. cf. *L. rueminiana*			**X**
Loranthaceae			
Loranthus obovatifolia			**X**
Santalaceae			
Viscum miquelii	**X**	**X**	
Viscum morlotii	**X**		**X**
Polygonaceae			
Polygonum leporimontanum		**X**	
Droseraceae			
Aldrovanda praevesiculosa		**X**	
Nyssaceae			
Nyssa altenburgensis	**X**		
Nyssa disseminata	**X**	**X**	
Nyssa cf. *haidingeri*	**X**		
Nyssa ornithobroma	**X**	**X**	**X**
Swida gorbunovii			**X**
Diplopanax limnophilum		**X**	
Eomastixia saxonica		**X**	**X**
Mastixia amygdalaeformis	**X**		
Mastixia lusatica		**X**	
Retinomastixia oertelii		**X**	

	late Oligocene	late Early Miocene	Late Miocene
Class or order / Family[1] / Fossil-species	Borna-Ost/Bockwitz TC[2]	Wiesa[3]	Wischgrund[4]
Pentaphylacaceae			
Eurya stigmosa	**X**	**X**	
Ternstroemia boveyana	**X**		
Ternstroemites bockwitzensis	**X**		
Theaceae			
Polyspora hradekense / *P. europaea*		**X**	
Symplocaceae			
Symplocos casparyi (*S. lignitarum*, *S. salzhausensis*)	**X**	**X**	**X**
Symplocos minutula		**X**	
Symplocos pseudogregaria		**X**	
Symplocos schereri		**X**	
Sphenotheca bornensis	**X**		
Sphenotheca incurva		**X**	**X**
Sphenotheca gigantea		**X**	
Pallioporia symplocoides		**X**	
Styracaceae			
Rehderodendron ehrenbergii		**X**	
Rehderodendron wiesaense		**X**	
Ericaceae			
aff. *Gaylussacia baccata*			**X**
Leucothoe narbonensis		**X**	
aff. *Vaccinium*			**X**
Oleaceae			
Fraxinus bilinica / *F. praedicta*			**X**
Fraxinus sp. aff. *F. excelsior*			**X**
Scrophulariaceae			
Limosella spuria	**X**		
Lamiaceae			
Collinsonia europaea	**X**		
Paulowniaceae			
Paulownia cantalensis		**X**	
Aquifoliaceae			
Ilex saxonica	**X**	**X**	
Ilex wiesaensis		**X**	
Asteraceae			
Taraxacum leporimontanum		**X**	
Ehretiaceae			
Ehretia hedericarpa	**X**		
Araliaceae			
Aralia dorofeevii	**X**		
Aralia longisperma	**X**		
Pentapanax tertiaries	**X**		
Schefflera dorofeevii	**X**		
Viburnaceae			
Sambucus lucida	**X**		
Dicotyledonae incertae sedis			
Carpolithus nitidus	**X**		
Dicotylophyllum spp.			**X**
Majanthemophyllum petiolatum	**X**		

Appendix II

Phytogeographical analysis of late Early Miocene Wiesa flora (Saxony, Germany): Revised list of fossil-taxa (App. I) and their supposed relationship with modern taxa (nearest living relatives/ecological equivalents) arranged to their present-day distribution area. If not indicated otherwise, taxa list was published by Mai 2000b. [1] system of gymnosperm families according to Christenhusz et al. 2011; system of angiosperm families according to APG IV 2016; [2] if not indicated otherwise, NLR stated by Mai 1999a, b, 2000a; [3] Kunzmann and Mai 2005; [4] Kunzmann 2014; [5] ecological equivalent; [6] distribution area partly in N. Africa; [7] Kvaček et al. 2015; [8] not *Illicium* after Oh et al. 2003, currently undeterminable due to insufficient preservation; [9] Africa and Australia; [10] Martinetto 2001; [11] only Asian distribution, not Australian; [12] Mai 1998; [13] Kvaček et al. 2002; [14] Kvaček et al. 2002; [15] Mai and Martinetto 2006; [16] Manchester and Fritsch 2014.

Class or order / family[1] / fossil-species	Nearest living relative[2]									
	E/SE Asia	N America	Disjunct E/ SE Asia – N America	Mediterranean	Macaronesia	Northern Hemisphere	Southern Hemisphere	Cosmopolitan	Extinct	Not applicable
Pteridophyta										
Pteridaceae										
"*Pteris*" *satyrorum*										**X**
Selaginellaceae										
Selaginella germanica								**X**		
Coniferophyta										
Pinaceae										
Abies resinosa				**X**[3]						
Cathaya bergeri / *C. roseltii*	*C. argyrophylla*[3]									
Keteleeria hoehnei	*K. davidiana*[3]									
Nothotsuga protogaea	*N. longibracteata*[3]									
Pinus grossana	*P. wallichiana*									
Pinus hampeana	*P. massoniana*									
Pityophyllum wiesaense									**X**	
Pseudolarix schmidtgenii	*P. amabilis*[3]									
Pseudotsuga jechorekiae	*P. sinensis*[4]									
Tsuga schmidtiana / *T. schneideriana*	*T. dumosa* / *T. sinensis*[3]									
Cupressaceae										
Quasisequoia couttsiae	*G. pensilis*[5]									
Sequoia abietina		*S. sempervirens*								
Tetraclinis salicornioides				*T. articulata*[6]						
Taxaceae										
Taxus engelhardtii	*T. mairei*[7]									
Torreya bilinica			**X**							
Ginkgophyta										
Ginkgoaceae										
Ginkgo adiantoides	*Ginkgo biloba*									
"Basal Dicots"										
Cabombaceae										
Brasenia victoria								**X**		
Nymphaeaceae										
Nuphar sp. cf. *N. canaliculatum*						**X**				
Schisandraceae										
"*Illicum*" *germanicum*[8]										**X**
Magnoliaceae										

Class or order / family[1] / fossil-species	Nearest living relative[2]									
	E/SE Asia	N America	Disjunct E/ SE Asia – N America	Mediterranean	Macaronesia	Northern Hemisphere	Southern Hemisphere	Cosmopolitan	Extinct	Not applicable
Magnolia ludwigii		*M. macrophylla*								
Liriodendron geminata	*L. chinensis*									
Liriodendron fragilis		*L. tulipifera*								
Magnolia sp. (folia)										**X**
Lauraceae										
Cinnamomum costatum	*C.* section *Camphora*									**X**
Daphnogene bilinica										**X**
Ocotea rhenana / *Laurophyllum pseudoprinceps*					*O. foetens*					
Laurinoxylon bergeri										**X**
Laurinoxylon endiandroid										**X**
Laurinoxylon hasenbergense										**X**
Laurinoxylon litseoides										**X**
Laurinoxylon microtracheale										**X**
Monocots										
Araceae										
Epipremnites reniculus									**X**	
Urospathites dalgasii									**X**	
Alismataceae										
Caldesia proventita										**X**
Alisma crassicarpum										**X**
Potamogetonaceae										
Potamogeton wiesaensis										**X**
Dioscoreaceae										
Dioscorea liblarensis								**X**		
Palmae										
Calamus daemonorops	*C.* spp.[9]									
Pontederiaceae										
Monochoria striatella	*M. plantaginea*									
Typhaceae										
Sparganium camenzianum										**X**
Sparganium haentzschelii										**X**
Sparganium nanum										**X**
Cyperaceae										
Carex limosioides										**X**
Dulichium marginatum										**X**
Scirpus khachlovii						**X**				
"Eudicots"										
Menispermaceae										
Sinomenium cantalense	*S. acutum*									
Sabiaceae										
Meliosma wetteraviensis	*M. veitchorum*, *M. alba*[10]									
Altingiaceae										
Liquidambar europaea				**X**						

Class or order / family[1] / fossil-species	Nearest living relative[2]									
	E/SE Asia	N America	Disjunct E/ SE Asia – N America	Mediterranean	Macaronesia	Northern Hemisphere	Southern Hemisphere	Cosmopolitan	Extinct	Not applicable
Corylopsis longehilata	*C.* spp.									
Distylium fergussonii	*D. racemosum*									
Fortunearia europaea	*F. sinensis*									
Vitaceae										
Ampelopsis malvaeformis	*A. delevayana, A .leeoides*									
Parthenocissus britannica	*P. henryana, P. thompsonii*									
Tetrastigma chandleri	*T.* spp. (*T. lanceolarium*)[11]									
Tetrastigma lobata	*T.* spp.[11]									
Vitis globosa	*V. thunbergii*									
Vitis lusatica						**X**				
Vitis palaeomuscadinia		*V. rotundifolia*								
Vitis teutonica	*V.* spp.									
Rosaceae										
Prunus leporimontana	aff. *P. serrulata*, *P. pseudocerasus*									
Prunus pereger	*P. kansuensis*, *P. ferganensis*									
Rubus laticostatus								**X**		
Sorbus herzogenrathensis	*S. foliolosa*									
Rhamnaceae										
Frangula solitaria						**X**				
Zizyphus striatus	*Z. incurva*[12]									
Ulmaceae										
Cannabaceae										
Gironniera carinata	*G.* spp.									
Trema lusatica			**X**							
Moraceae										
Ficus potentilloides								*F. carica*		
Urticaceae										
Boehmeria raria										**X**
Fagaceae										
Quercus rhenana										**X**
Quercus sp. (folia)										**X**
Trigonobalanopsis exacantha / rhamnoides	*Formanodendron doichangensis*									
Myricaceae										
Myrica boveyana (= *M. wiesaensis*)	*M. javanica*									
Myrica ceriferiformis		*M. pensylvanica*								
Myrica stoppii	*M. nagi*, *M. rubra*									
Myrica suppanii							*M. cordifolia*			
Juglandaceae										
Carya bohemica		*C. aquatica*								
Carya hauffei		*C. aquatica*								
Carya lusatica										**X**
Cyclocarya cyclocarpa	*C. paliurus*									
Engelhardia orsbergensis	*E. roxburghiana*									
Betulaceae										

Class or order / family[1] / fossil-species	Nearest living relative[2]									
	E/SE Asia	N America	Disjunct E/ SE Asia – N America	Mediterranean	Macaronesia	Northern Hemisphere	Southern Hemisphere	Cosmopolitan	Extinct	Not applicable
Passifloraceae										
Passiflora kirchheimeri							*P. aurantiaca*			
Euphorbiaceae										
Acalypha fragilis		*A. virginica*, *A. caroliniana*								
Sapium germanicum	*S. sebiferum*									
Combretaceae										
Quisqualis pentaptera (?*Craigia bronnii*)[12]	(*Craigia kwangsiensis*)[13]									
Lythraceae										
Decodon gibbosus / *Microdiptera menzelii*		*D. verticillatus*								
Staphyleaceae										
Turpinia ettingshausenii	*T. formosana*, *T. pomifera*, *T. montana*									
Rutaceae										
Phellodendron lusaticum	*P.* spp.									
Toddalia maii	*T. asiatica*									
Malvaceae										
Burretia instructa	(*Craigia* or *Tilia*[14])								**X**	
Santalaceae								**X**		
Viscum miquelii										**X**
Polygonaceae										
Polygonum leporimontanum	aff. *P.* section *Pleuropterus*									
Droseraceae										
Aldrovanda praevesiculosa								**X**		
Nyssaceae										
Nyssa disseminata		*N. sylvatica*								
Nyssa ornithobroma		*N. aquatica*								
Eomastixia saxonica									**X**	
Diplopanax limnophilum	*D. stachyanthus*									
Mastixia lusatica	*M.* spp.									
Retinomastixia oertelii									**X**	
Tectocarya elliptica									**X**	
Pentaphylacaceae										
Eurya stigmosa	*E. japonica*									
Theaceae										
Polyspora hradekense / *europaea*	*P.* spp.									
Symplocaceae										
Symplocos casparyi *S. lignitarum*, *S. salzhausensis*	*S. sulcate* (*macrophylla*), *S. ophirensis*[15]									
Symplocos minutula			**X**[15]							
Symplocos pseudogregaria	*S. anomala*, *S. tingifera*, *S. kuroki*[15]									
Symplocos schereri	*S. tankae*, *S. costata*, *S. crassilimba*, *S. cerasifolia*[15]									
Sphenotheca incurve	extant Asian *Symplocos* spp.[16]									

Class or order / family[1] / fossil-species	Nearest living relative[2]									
	E/SE Asia	N America	Disjunct E/ SE Asia – N America	Mediterranean	Macaronesia	Northern Hemisphere	Southern Hemisphere	Cosmopolitan	Extinct	Not applicable
Pallioporia symplocoides									**X**[16]	
Styracaceae										
Rehderodendron ehrenbergii	*R.* spp.									
Rehderodendron wiesaense	*R. kwangtungense*									
Ericaceae										
Leucothoe narbonensis										**X**
Paulowniaceae										
Paulownia cantalensis	*P.* spp.									
Aquifoliaceae										
Ilex saxonica					*I. perado*					
Ilex wiesaensis		*I. ambiqua*								
Asteraceae										
Taraxacum leporimontanum								**X**		

Appendix III

Phytogeographical Reference Region Assessment (PRRA): R script written with R® software package for drawing reference region maps in grid box illustration style; needed ocean mask (natural-earth-vector) can be downloaded from https://github.com/nvkelso/natural-earth-vector/blob/master/110m_physical/ne_110m_ocean.shp

```
# Author: Shufeng Li, Xishuangbanna Tropical Botanical Garden, Chinese Academy of Sciences (XTBG, CAS)
# Date: Oct. 20, 2021
# Contact: lisf(at)xtbg.org.cn
# PURPOSE OF THIS PROGRAM---
# This Phytogeographic Reference Region Assessment (PRRA) approach is to find similarity between a (fossil) flora and modern vegetation or biodiversity.
# The similarity between taxa list of nearest living relatives from a (fossil) flora and modern GBIF data were calculated, the high similarity values
# represent high level of similarity between a (fossil) flora and GBIF data, thus the vegetation of the high value grids can be considered
# as the vegetation type of the (fossil) flora, it can also indicate the biodiversity similarity between a (fossil) flora and modern GBIF data.

library(maptools)
data(wrld_simpl) # this data from maptools package
library(raster)
library(colorRamps)
library(dplyr) # for %T>% pipe
library(purrr) # for imap
library(readr) # for write_tsv
library(magrittr) # for %T>% pipe
library(rgbif) # for occ_download
library(taxize) # for get_gbifid
library(data.table) # for fread

##read taxa name nearest living relatives
setwd(,.../.../...') # set the working direction
taxa <- read.csv(„taxa list of fossil flora.csv“,header = TRUE)
#The taxa list of fossil flora have two columns
#The first column named Rank which should have the class of taxa, i.e.,“family“,“genus“ or „species“.
#The second column named Taxa which should have the taxa list of nearest living relatives.

fieldsvalue = c(,decimalLongitude‘,‘decimalLatitude‘,‘family‘,‘genus‘,‘species‘,‘basisOfRecord‘)
# fill in your gbif.org credentials
user <- „***“ # your gbif.org username
pwd <- „***“ # your gbif.org password
email <- „***@***“ # your email

taxa$Rank<-tolower(taxa$Rank)
myspecies<-as.vector(taxa$Taxa )
rank_family<-as.vector(taxa[which(taxa$Rank==‘family‘),])
rank_genus<-as.vector(taxa[which(taxa$Rank==‘genus‘),])
rank_species<-as.vector(taxa[which(taxa$Rank==‘species‘),])
# match the names
gbif_taxon_keys <-
  myspecies %>% # use fewer names if you want to just test
  taxize::get_gbifid_(method=“backbone“) %>% # match names to the GBIF backbone to get taxonkeys
  imap(~ .x %>% mutate(original_sciname = .y)) %>% # add original name back into data.frame
  bind_rows() %T>% # combine all data.frames into one
  write_tsv(path = „all_matches.tsv“) %>% # save as side effect for you to inspect if you want
  filter(matchtype == „EXACT“ & status == „ACCEPTED“) %>% # get only accepted and matched names
  filter(kingdom == „Plantae“) %>% # remove anything that might have matched to a non-plant
  pull(usagekey) # get the gbif taxonkeys

res<-occ_download(
  pred_in(„taxonKey“, gbif_taxon_keys),
  format = „SIMPLE_CSV“,
  user=user,pwd=pwd,email=email
)

occ_download_meta(res)
```

```
x <- occ_download_list(user=user,pwd=pwd)
x$results <- tibble::as_tibble(x$results)
x

#read the download GBIF data
data<-fread(„.../.../.../the_download_data.csv“,header=T,sep=“\t“, dec=“.“,quote=““,select=fieldsvalue)
##show how to cite the gbif data
# occ_download_meta(res) %>% gbif_citation()
# occ_download_get(„0000796-171109162308116“) %>% gbif_citation()

#Cleaning the data
data1<-data[data$basisOfRecord==‘PRESERVED_SPECIMEN‘,]
dim(data1)
colnames(data1)
##conduct some procedures to clean the data
dups2 <- duplicated(data1[, c(‚species‘,‘decimalLongitude‘,‘decimalLatitude‘)]) # find the duplicate data based on the coordinates
sum(dups2) # how many of duplicate data
data2<- data1[!dups2, ] #remove duplicate data
data2<-subset(data2, !(is.na(decimalLongitude)|is.na(decimalLatitude))) # delete some missed coordinates

#check if there are some data swapped the latitude and the longitude
data2matrix<-as.data.frame(data2)
data2matrix[(data2matrix$decimalLatitude > 90) & (data2matrix$decimalLongitude < 90), c(„decimalLongitude“, „decimalLatitude“)] <-
data2matrix[(data2matrix$decimalLatitude > 90) & (data2matrix$decimalLongitude < 90), c(„decimalLatitude“, „decimalLongitude“)]
data3<-data2matrix
# the following codes is to find some mismatch
coordinates(data3) <- ~decimalLongitude+decimalLatitude
range(data2matrix$decimalLongitude)
range(data2matrix$decimalLatitude)
crs(data3) <- crs(wrld_simpl)
class(data3)
class(wrld_simpl)
ov <- over(data3, wrld_simpl)
cntr <- ov$NAME
i <- which(is.na(cntr))
if (length(i)!=0){
 data3<-data3[-i,] #if i is 0, then not run this line
}

data4<-as.data.frame(data3,row.names = NULL)

# Copy family, genus and species name to column rank
data4[,“rank“] <- NA
data4[which(data4$family%in%rank_family$Taxa), „rank“] <-data4[which(data4$family%in%rank_family$Taxa), „family“]
data4[which(data4$genus%in%rank_genus$Taxa), „rank“] <-data4[which(data4$genus%in%rank_genus$Taxa), „genus“]
data4[which(data4$species%in%rank_species$Taxa), „rank“] <-data4[which(data4$species%in%rank_species$Taxa), „species“]

##to show the data on global map
# plot(wrld_simpl,col=‘light yellow‘)
# box() ## restores the box around the map
# points(data4$decimalLongitude , data4$decimalLatitude, col=‘blue‘, pch=20, cex=0.9)

## below codes are used to calculate the similarity
data4[„rank“] <- lapply(data4[„rank“], as.factor)
spec.lev<-levels(data4$rank)
spec.lev
r <- raster(xmn=-180, ymn=-90, xmx=180, ymx=90, res=2) # resolution can be changed according to your need, but 2 degree is suggested
proj4string(r)<-CRS(„+proj=longlat +datum=WGS84“)
z <- raster(xmn=-180, ymn=-90, xmx=180, ymx=90, res=2) # resolution can be changed according to your need, but 2 degree is suggested
proj4string(z)<-CRS(„+proj=longlat +datum=WGS84“)
```

```
values(z)<-0
data5<-data4
coordinates(data5) <- ~decimalLongitude+decimalLatitude
proj4string(data5) <- proj4string(r)
for (i in 1:length(spec.lev)){
data6<-data5[which(data5$rank==spec.lev[i]), ]
count <- rasterize(data6, r, fun='count')
count[which(count@data@values<1)] <-0 #samples less than  1 then consider it is zero
count[which(count@data@values>=1)] <-1 #samples larger than 0 then consider there is this taxa
count<-(count[[2]])#there are two layers, we need choose one layer
count[is.na(count[])] <- 0 # assign o to NA value, otherwise it will only have NA in Z
z<-z+count
}

#set colors
colfunc<-colorRampPalette(c("green3","yellow","red3"))
#plot(rep(1,50),col=(colfunc(50)), pch=19,cex=2)
##plot global map
my_window <- extent(-180,180,-90,90)
lon_seq <- seq(-180, 180, by = 30)
lat_seq <- seq(-60, 60, by = 30)
lon_lab<- parse(text = paste(lon_seq, "*degree", sep = ""))
lat_lab<- parse(text = paste(lat_seq, "*degree", sep = ""))

plot(z)
writeRaster(z, filename="biodiversity_d2_genus" , format="ascii", overwrite=TRUE)

##read ocena_mask, it can be download from https://github.com/nvkelso/natural-earth-vector/blob/master/110m_physical/
ne_110m_ocean.shp
ocean_mask<-shapefile("/.../.../ne_110m_ocean.shp")
proj4string(ocean_mask)<-CRS("+proj=longlat +datum=WGS84")

##starts the graphics device driver for producing PDF graphics
pdf(file='map_similariy_global.pdf',height=8, width=11)
par(mgp=c(0,0.3,0),mar=par()$mar+c(0,0,0,2),oma=c(0,0,0,0))
plot(z,col=colfunc(100),ext=my_window,box = FALSE,
    xlim=c(-180, 180),ylim=c(-90, 90),axes = FALSE,
    legend.args = list(text = ,similarity', side = 4,
                line = 2.5, cex = 1))
plot(ocean_mask,col="blue",add=TRUE,lwd = 0.2)
axis(1,lty = 1, lwd = 1,at=lon_seq,labels =lon_lab,pos=-90,tck=-0.01)
axis(2,lty = 1, lwd = 1,at=lat_seq,labels =lat_lab,pos=-180,tck=-0.01)
axis(3,lty = 1, lwd = 1,at=lon_seq,labels =lon_lab,pos=90,tck=-0.01)
axis(4,lty = 1, lwd = 1,at=lat_seq,labels =lat_lab,pos=180,tck=-0.01)
dev.off()

##plot regional map
my_window <- extent(50,160,-10,60)
oceancrop<-crop(ocean_mask, extent(50,160,-10,60))
zcrop <- crop(z, extent(50,160,-10,60))
##starts the graphics device driver for producing PDF graphics
pdf(file='map_similariy_Asian.pdf',height=8, width=11)
par(mgp=c(0,0.3,0),mar=par()$mar+c(0,0,0,2),oma=c(0,0,0,0))
plot(zcrop,col=colfunc(100),ext=my_window,box = FALSE,
    xlim=c(50, 160),ylim=c(-10, 60),axes = TRUE,
    legend.args = list(text = ,similarity', side = 4,
                line = 2.5, cex = 1))
plot(ocean_mask,col="blue",add=TRUE,lwd = 0.2)
dev.off()
```

Appendix IV

Results for IPR Similarity Analysis and Taxonomic Similarity (TS) for late Early Miocene Wiesa flora, eastern Germany revealed by application of Drudge 1 and 2 online tools (Teodoridis et al. 2020, 2021). Abbreviations: MDiff – mathematical difference; TDiff – total difference. IPR Vegetation Analysis score sheet deposited in freely accessible database (Teodoridis et al. 2011–2021) at http://www.iprdatabase.eu.

IPR Similarity – Drudge 1

Fossil / modern plant assemblages	**BLD**	**BLE**	**SCL+LEG**	**MDiff**
Wiesa	45.16%	45.97%	8.87%	-
Broad-leaved Evergreen Sclerophyllous Forest (Guizhou)	44.00%	47.43%	3.43%	6.74%
C45: West Low Caucasian krummholz and open woodlands (*Betula litwinowii*, *Fagus sylvatica* subsp. *orientalis*, *Acer trautvetteri*) with *Quercus pontica*, *Betula medwediewii*, scrub (*Rhododendron caucasicum*) with *Rhododendron ungernii*, tall-herb communities (*Ligusticum alatum*, *Milium schmidtianum*) with *Heracleum cyclocarpum*, *Heracleum mantegazzianum* and grasslands (*Agrostis planifolia*, *Geranium platypetalum*) with *Euphorbia oblongifolia*, *Astragalus bachmarensis*	24.75%	29.70%	2.97%	7.14%
Yakushima Island – Mixed Mesophytic forest – *Eurya-Cryptomeria japonica* assoc., *Tsuga sieboldii* subassoc.	19.98%	19.69%	6.82%	7.17%
H1: Colchic lowland to submontane mixed oak forests (*Quercus imeretina*, *Quercus hartwissiana*, *Zelkova carpinifolia*, *Carpinus betulus*, *Castanea sativa*, *Fagus sylvatica* subsp. *orientalis*) with evergreen understorey species (*Rhododendron ponticum*, *Prunus laurocerasus*), alternating with oak and hornbeam-oak forests (*Quercus iberica*, *Carpinus betulus*) in the submontane belt	28.73%	26.02%	2.17%	7.34%
C42: Southwest Caucasian krummholz and open woodlands (*Betula litwinowii*, *Fagus sylvatica* subsp. *orientalis*, *Acer trautvetteri*) with *Betula megrelica*, *Quercus pontica*, scrub (*Rhododendron caucasicum*) with *Rhamnus imeretina* (on carbonate rocks with *Corylus colchica*), tall-herb communities (*Heracleum ponticum*) with *Delphinium pyramidatum* (on carbonate rocks with *Heracleum aconitifolium*, *Ligusticum arafoe*) and grasslands (*Calamagrostis arundinacea*, *Stachys macrantha*, on carbonate rocks with *Geum speciosum*, *Carex pontica*)	24.88%	18.43%	3.69%	10.35%

IPR Similarity – Drudge 2

Fossil / modern plant assemblages	**BLD**	**BLE**	**SCL+LEG**	**D-HERB**	**M-HERB**	**MDiff**
Wiesa	33.94%	34.55%	6.67%	0.61%	4.24%	-
Montane Coniferous Forest – Taiwan	23.80%	31.70%	1.91%	1.44%	12.44%	14.19%
Broad-leaved Evergreen Sclerophyllous Forest – Pine Forest (Yunnan)	49.90%	33.30%	4.10%	0.41%	2.05%	16.36%
Broad-leaved Evergreen Sclerophyllous Forest (Guizhou)	44.00%	47.43%	3.43%	0.00%	0.00%	17.20%
D43: Northeast European open hygrophilous pine forests (*Pinus sylvestris*) with bog mosses and dwarf shrubs, with *Chamaedaphne calyculata*, *Eriophorum vaginatum*	33.12%	18.03%	10.64%	0.00%	12.74%	19.02%
Mt. Fuji - Broad-leaved Evergreen Forest – *Camellia japonica* region	51.97%	40.13%	2.63%	0.00%	5.26%	19.34%

Taxomonic Similarity – Drudge 1 and 2

Fossil / modern plant assemblages	**TS**
Wiesa	-
Mixed Mesophytic Forest – Tianmu-Shan (Zhejiang)	25.53%
Broad-leaved Deciduous Forest (Eastern Guizhou)	25.53%
Mixed Mesophytic Forest – Southern Anhui	25.53%
Mt. Fuji – Broad-leaved Deciduous Forest – *Fagus crenata* region	25.53%
Mt. Fuji – Broad-leaved Deciduous Forest – *Vaccinium-Picea* region	24.47%

Mix – Drudge 1

Fossil / modern plant assemblages	BLD	BLE	SCL+LEG	MDiff	TS	TDiff
Wiesa	45.16%	45.97%	8.87%	-	-	-
Broad-leaved Evergreen Sclerophyllous Forest (Southern Hunan)	52.07%	42.01%	0.00%	13.57%	21.28%	79.88%
Broad-leaved Evergreen Sclerophyllous Forest (Northern Guangxi)	52.07%	42.01%	0.00%	13.57%	21.28%	79.88%
Broad-leaved Deciduous Forest (Eastern Guizhou)	60.17%	24.68%	0.20%	31.89%	25.53%	81.01%
Montane Coniferous Forest – Taiwan	23.80%	31.70%	1.91%	11.39%	19.15%	81.65%
Broad-leaved Evergreen Sclerophyllous Forest (Fujian)	23.45%	59.91%	2.27%	30.50%	23.40%	82.45%

Mix – Drudge 2

Fossil / modern plant assemblages	BLD	BLE	SCL+LEG	D-HERB	M-HERB	MDiff
Wiesa	33.94%	34.55%	6.67%	0.61%	4.24%	-
Broad-leaved Deciduous Forest (Eastern Guizhou)	60.17%	24.68%	0.20%	0.00%	0.00%	29.08%
Broad-leaved Evergreen Sclerophyllous Forest (Southern Hunan)	52.07%	42.01%	0.00%	0.00%	0.00%	21.15%
Broad-leaved Evergreen Sclerophyllous Forest (Northern Guangxi)	52.07%	42.01%	0.00%	0.00%	0.00%	21.15%
Broad-leaved Evergreen Sclerophyllous Forest (Fujian)	23.45%	59.91%	2.27%	0.00%	0.00%	28.13%
Montane Coniferous Forest – Taiwan	23.80%	31.70%	1.91%	1.44%	12.44%	14.19%